U.S. DEPARTMENT OF THE INTERIOR
U.S. GEOLOGICAL SURVEY

Physical Processes of Shallow Mafic Dike Emplacement Near the San Rafael Swell, Utah

by

Paul T. Delaney [1] and Anne E. Gartner [2]

Open-file Report 95-491

1 U.S. Geological Survey
2255 North Gemini Drive
Flagstaff, Arizona, 86001
520/556-7270, fax -7169
delaney@aa.wr.usgs.gov

2 U.S. Geological Survey
345 Middlefield Road
Menlo Park, California, 94025
415/329-5209, fax -5203
aegartne@mojave.wr.usgs.gov

1995

CONTENTS

ABSTRACT

Some 200 shonkinite dikes, sills, and breccia bodies are exposed on the western Colorado Plateau between the Waterpocket monocline and San Rafael Swell of south central Utah. Potassium-Argon ages cluster at about 3.7 and 4.6 Ma, contemporaneous with mafic volcanism along the nearby plateau margin, which the swarm parallels. Dike thicknesses range upward to about six meters, with the thickness distribution having a log-normal mean of 105 cm. Most of the dikes are less than one kilometer long in outcrop, the longest being nine kilometers. The shonkinite magmas were primitive and probably ascended directly from mantle depths. Outcrop lengths of the San Rafael dikes, therefore, are much less than their heights, implying that the present exposures lie along the irregular upper periphery of dikes that lengthen and merge at depth. Orientations of offsets along dike contacts record local directions of dike-fracture propagation; about one half of the measurements of these directions plunge less than 30°, showing that lateral propagation at the dike periphery is as important as the vertical propagation that is ultimately responsible for ascent. The San Rafael dikes are exposed at shallow depth and appear to thicken upward. Probably, vesiculation of the shonkinite magmas enhanced the pressure difference responsible for dilation; propagation likely ceased when the first dike segments began to feed nearby sills or vented to initiate small-volume eruptions.

Most of the dikes are exposed in clastic strata of the Jurassic San Rafael Group; they probably acquired their strikes, however, while ascending along well-developed joint sets in massive sandstones of the underlying Glen Canyon Group. Rotation of far-field stresses during the emplacement interval cannot account for disparate strikes of the dikes, which vary through 110°, most lying between N25°W and N0°E. Rather, the two regional horizontal principal stresses were probably nearly equal, and so the dominant N76°E direction of dike opening was not strongly favored. Across the center of the swarm, about 10 to 15 dikes overlap and produce about 17 m of total dike-swarm dilation. Many are in sufficient proximity that later dikes should be thinner than earlier ones if neither the magma-driving pressure

nor regional stresses were changing during the emplacement interval. Yet, dike thicknesses do not vary systematically either along the length of the swarm or in proportion to the number of neighboring dikes. Probably, therefore, regional extension during the magmatic interval relieved localized compressive stresses generated by dike emplacement.

INTRODUCTION

A Pliocene dike swarm, almost 60 km long and nowhere more than 30 km wide, is exceptionally well exposed near the western margin of the Colorado Plateau of south-central Utah (Figures 1, 2). The dikes are mostly one meter thick and have almost 275 km of linear outcrop within nearly flat-lying clastic strata of the Jurassic San Rafael Group. Breccia bodies and plug-like intrusions are present along some of the dikes. Together, they fed sills exposed in the same strata and, probably, eruptive rocks now removed by no more than about two kilometers of erosion. The igneous rocks are alkalic, predominantly shonkinites cooled from primitive, mantle-derived magma. The San Rafael intrusions likely exemplify the shallow subsurface beneath volcanic fields of mafic maars, cinder cones, and small-volume lava flows such as are common throughout western North America.

This paper summarizes observations and measurements collected to constrain some physical processes of mafic dike emplacement in a setting of relatively simple igneous and host-rock geology. We report on length, thickness, strike, and dip of dikes and on the character and strike of systematic joints in strata of the San Rafael Group and the Navajo Sandstone of the underlying Glen Canyon Group. We also report on directions of dike-fracture propagation. These measurements characterize the means of magma ascent and the ambient state of regional stress and accompanying crustal extension during the magmatic interval, which lasted for about a million years.

GEOLOGIC SETTING

Tectonics

The San Rafael dike swarm trends roughly parallel with the nearby boundary of the Colorado Plateau and the Basin and Range provinces about 20–50 km to the west (Figure 1). The swarm lies between the Waterpocket monocline and the anticlinal San Rafael Swell, although it parallels neither of these Laramide folds nor any other nearby flexures and faults (Figure 2). The mean N14°W strike of the dikes approximately parallels an inferred N20°W direction of fractures in Precambrian basement of the Colorado Plateau (Davis, 1978); the trend of the northern laccolithic intrusions of the Henry Mountains and of the Henry Basin to the south-southeast, for example, are aligned with the San Rafael swarm along this direction (Figure 1).

The San Rafael intrusions resemble other Tertiary mafic alkaline rocks that crop out in sparse, widely spaced groups along the western margin of the North American craton. Such rocks are locally exposed along the transition zone between the Colorado Plateau and Basin and Range provinces (Thompson and Zoback, 1979; Kempton and others, 1991) and have been discussed most recently by Tingey and others (1991); the nearest, the minette and melanephelinites of the Wasatch Plateau, are about 40–80 km north of the San Rafael swarm (Figure 1). Much of the southern and western Colorado Plateau margin has been the locus of volcanism since the Tertiary; the San Rafael swarm lies at the northeastern limit of the northeast trending St. George volcanic zone (Smith and Luedke, 1984) that crosses onto the Plateau from the Basin and Range province of southern Utah (Figure 1). Although volcanism along this zone began in the early Oligocene, later activity produced Pliocene and Quaternary alkalic and tholeiitic basaltic rocks of the High Plateaus (Mattox, 1991, 1994), adjacent to the Colorado Plateau.

Judging from the primitive nature of the shonkinites, they ascended directly from a source region in the mantle. Indeed, no geophysical anomaly has been identified near the San Rafael swarm to suggest a crustal magma reservoir. The swarm lies on the flanks of an elongate regional aeromagnetic high and a positive Bouger-gravity anomaly identified from locally sparse data (Zietz and others, 1976; Cook and others, 1989). The nearby aeromagnetic high extends northeasterly from the Waterpocket monocline to the San Rafael anticline; the gravity anomaly is centered over the San Rafael anticline.

Plateau uplift was waning when the dikes were emplaced at about 4 Ma (Thompson and Zoback, 1979) and much of the post-Mesozoic strata was already stripped by erosion. Dikes at 2200–2600-m elevations on the west side of the San Rafael swarm are within six kilometers of lavas of similar age and composition at elevations above 3000 m (Nelson, 1989). The swarm lies as much as 30 km east of the these lavas, at elevations as low as 1500 m. Although no paleotopographic reconstruction is available, modern exposures probably correspond to no more than about 2 km of emplacement depth.

Igneous Rocks

All of the exposed dike rocks are dark gray, locally porphyritic, micro-shonkinites containing clinopyroxene, biotite, sanidine, olivine, and magnetite, with accessory analcite and zeolites. SiO_2 ranges from 44 to 48 weight percent and total alkalis range from 5.2 to 7.2 percent (Gilluly, 1927; Williams, 1983; Gartner, 1986). The shonkinites are primitive, with magnesium numbers of 0.72 to 0.75. Like other primitive alkaline rocks along the western margin of the North American craton, the San Rafael magmas probably originated in a mantle region of low partial melt and did not fractionate during ascent (Tingey and others, 1991).

Because of the field relations and similar compositions of the San Rafael dikes and sills, Gilluly (1927) concluded that they were contemporaneous and comagmatic. Syenites in the sills are present as lenses, globules, and veins formed from residual magma during fractional crystallization of the shonkinitic liquid. Williams (1983) found evidence for a silicate-liquid immiscibility gap between the shonkinitic and syenitic liquids. The sills number about a dozen and are nowhere thicker than 30 m.

Alteration of the shonkinites is pervasive. Their groundmass is typically chloritic, and calcite and zeolites, mostly thomsonite, fill veins and abundant vesicular and amygdaloidal cavities, and also replace of phenocrysts. Gypsum is locally found in veins. Contact metamorphism of sedimentary wall rocks has been locally identified along many dikes, and it is pervasive along the sills.

About 45 dikes contain abundant breccias of admixed shonkinite and comminuted host rock (Gartner and Delaney, 1988). In most instances, brecciation was accompanied by wall-rock erosion, leading to local widening of dikes during magma flow. The resulting structures are best called breccia pipes and plugs. Although they probably merged upward to volcanic necks, now removed by erosion, no undoubted scoria, tephra, agglutinate, or tuffaceous facies of the shonkinites were identified.

Age of Intrusion

We used K-Ar methods to determine that the age of the San Rafael swarm is about 4 Ma (Tables 1 and 2). Seven samples collected from four dikes, a breccia body, and a sill yielded ages ranging from 3.4±0.2 to 4.7±0.3 Ma. Ages ranging from 3.8±0.2 to 6.4±0.4 Ma were determined from four trachybasalt and basaltic andesite flows at higher elevations west of the swarm (Figure 2). Thus, dike emplacement was contemporaneous with some of the nearby volcanism.

Ages of the intrusive rocks fall into two groups, with three samples ranging from 3.4±0.2 to 3.8±0.2 Ma and four samples ranging from 4.6±0.2 to 4.7±0.3 Ma. The youngest radiometric age, 3.4±0.2 Ma, was obtained from a sample (SAL-2) collected from the same dike as another sample (SAL-1A) with an age of 3.8±0.2 Ma. Within the analytic uncertainty of the modest number of samples, magmatism may have been confined to only two periods, a little more than one million years apart. Two other samples yielded $^{40}Ar/^{39}Ar$ ages of 5.2±0.4 and 6.6±0.7 Ma (Tingey and others, 1991). These determinations, however, lack plateaus in their age spectrums and are not isochronous on inverse-correlation plots (S. Nelson, pers. comm., 1995).

Host Strata

The great majority of intrusions are exposed in Middle Jurassic strata of the San Rafael Group, consisting of the Carmel Formation, Entrada Sandstone, and Curtis and Summerville Formations (Gilluly, 1929; Smith and others, 1963). These rocks are mostly near-shore clastic marine deposits, dominantly fine-grained sandstones and siltstones and commonly cemented with interstitial calcite. Their overall thickness is about 550 m. A few dikes are exposed in the lowermost strata of the Late Jurassic Morrison Formation, which unconformably overlies the San Rafael Group. A few other dikes, at higher elevations along the westernmost margin of the swarm, are exposed in the Cretaceous Mancos Shale (Figure 2; Nelson, 1989). Exposures of intrusions in the San Rafael Group and Morrison Formation are generally good or excellent; we are confident that virtually all dike segments cutting these units were identified in the course of our work.

Some intrusions are traceable down to the underlying Triassic (?) and Jurassic Navajo Sandstone of the Glen Canyon Group. The Navajo Sandstone unconformably underlies the Carmel Formation and consists of massive beds of eolian origin. Thickness of the Navajo Sandstone is about 250 m. The Glen Canyon Group is comprised dominantly of massive sandstones and has a thickness of about 450 m. Difficult access in the Navajo Sandstone and accumulations of sand in the slot canyons left by rapid weathering of the dikes made them difficult to examine. Our observations suggest that far fewer dike segments are exposed there than in the overlying strata.

DIKE FORM

Thickness

Thickness varies appreciably along most dike segments, so that they are generally thickest near their centers and thinnest near their tips. A total of 287 measurements were obtained from the thickest outcrops at each locality. Some dike segments are locally anomalously thick owing to brecciation and erosive removal of wall rocks (Delaney and Pollard, 1981) or to overlapping of adjacent segments or offsets (Pollard and others, 1975, 1982). We do not include these among our data.

The median dike thickness is 110 cm and ranges from 10 to 650 cm in a fashion that is not Gaussian, or normally distributed. Some dikes, for instance, are a couple meters thicker than the median, but none can be a couple meters thinner. Accordingly, we calculated log-normal mean thicknesses of dikes in the Carmel Formation, Entrada Sandstone, and Curtis and Summerville Formations (Figure 3). The log-normal mean thickness of dikes in the Carmel Formation is 119 cm. The thickest dikes are in the Carmel Formation, and thickest among these are near its base. Log-normal mean thicknesses of dikes in the Entrada Sandstone and Curtis and Summerville Formations are 92 and 97 cm, respectively. The log-normal mean of all thickness measurements of dikes in the San Rafael Group is 105 cm.

Length

A total of 1942 dike segments, ranging in outcrop length from about 25 to 2140 m, can be distinguished on the 1:48,000-scale map of the San Rafael swarm (Gartner and Delaney, 1988), which includes all dikes exposed in the San Rafael Group and Morrison Formation and excludes those exposed in the underlying Navajo Sandstone and overlying Mancos Shale. Although we are confident of having found virtually all dikes exposed in the strata of the San Rafael Group, more segments would be distinguished at larger map scales because segmentation occurs at virtually all sizes down to the narrowest segments. An inverse logarithmic relation exists between segment lengths and their frequency of occurence for segments between 25 m and about 1250 m in length (Figure 5a). The three longest dike segments in the San Rafael swarm do not fit this simple relation. At larger map scales, it would be apparent that these segments--in fact, most segments--are not single but multiple. Thus, the particular relation between segment length and frequency of occurence portrayed in Figure 5a would not be reproduced from data compiled at smaller or larger scales.

Dike segments are not everywhere arranged *en echelon*. In fact, their arrangement is so irregular that we are unable to uniquely determine the number of dikes in the San Rafael swarm. One of the areas of greatest intrusive density shows more than 250 segments after compilation at a scale of 1:48,000 (Figure 4). We grouped these segments into 13 dikes. By a similar grouping of segments, the entire San Rafael swarm comprises 174 dikes. The log-normal mean dike-outcrop length is one kilometer (Figure 5b); many dikes are only several hundred meters long and so the distribution of thicknesses is skewed toward shorter lengths. One dike has 50 segments and several have only one.

Determinations of the number of San Rafael dikes are qualitative. In spite of, or even because of, the excellent exposures, other workers would likely group the segments somewhat differently. Moreover, dike length is probably greatly dependent upon erosional level; many of the San Rafael dikes likely merge with others below the present exposures.

Orientation

Virtually all dikes consist of numerous segments (Pollard and others, 1975, 1982), each separated from its neighboring segments by host rocks. Arrangements of segments can be irregular, although commonly idealized by an echelon pattern, both in the sense and distance of offset. Strikes of the San Rafael dikes were measured by their azimuth from one tip to the other without regard to its outcrop pattern in between; this measure of strike can vary appreciably from strikes of dike segments. Most of the San Rafael dikes strike from about N25°W to N0°E (Figure 6); the full range spans 110° of azimuth from N85°W to N25°E. Both the median and mean strikes are N14°W, oblique to the trend of the swarm.

Dips of dikes were measured where exposures permitted. The 79 measurements reveal dips typically more steep than 80°, with no marked preference for easterly or westerly dip directions (Figure 6). The median and mean dip is 89° westward.

Relation between thickness and length

Dikes emplaced in the same setting, with similar host rocks and similar magmas should, in principle, possess a relation between maximum thickness and length that can be expressed by results from linear elastic fracture mechanics, as follows. Dilatant cracks propagate when the fracture toughness K_I^{crit} of the surrounding solid is exceeded by the stress intensity K_I at the crack tip (Broek, 1978). A uniformly pressurized crack growing quasistatically in an elastic medium (Figure 7a) maintains a relation among maximum thickness T_{max} half-length L, driving pressure $P_m - S_h$, the difference between magma pressure P_m and the far-field compressive stress acting normal to the crack S_h, and elastic constants of the medium, μ and ν, the shear modulus and Poisson's ratio. We have:

$$
\begin{aligned}
&P_m > S_h \\
&T_{max} = \frac{P_m - S_h}{\mu / (1-\nu)} L \\
&K_I^{crit} = K_I = (P_m - S_h)\sqrt{L}
\end{aligned}
\qquad (1)
$$

(Pollard and Segall, 1987). As dilatant cracks grow longer, maintaining $K_I^{crit} = K_I$, they propagate at lower driving pressure, which is why dike propagation is energetically favorable. It is also favorable that a crack be oriented perpendicular to the direction of least compressive stress. Log-normal means of dike thicknesses and lengths are about one meter and one kilometer (Figures 3, 5b), respectively. Equations 1 predicts that for dike-aspect ratios of $T_{max} / L \approx 10^{-3}$ and for stiffnesses of $\mu / (1-\nu) = 5\,\text{GPa}$, driving pressures would be $P_m - S_h \approx 5\,\text{MPa}$; these estimates yield fracture toughnesses of $K_I^{crit} \approx 150\,\text{MPa}\sqrt{\text{m}}$. This estimate far exceeds values measured in the laboratory, as has been discussed by Rubin (1993), among others.

To see if equations 1 could be used to constrain those parameters in equations 1 relating dike thickness and length, we plotted lengths of the 85 San Rafael dikes with thickness measurements (Figure 8a). Assuming that ν, μ, and K_I vary negligibly among the host rocks, equations 1 predict that $T_{max} \propto \sqrt{L}$. This relation is not supported by the data.

Relations among thickness, length, strike

Dike-opening displacement might display a dependency on the regional stress resolved on the dike wall if there exist pre-existing planes of weakness, such as joints, to guide dikes into orientations other than that perpendicular to the direction of least compressive stress and if the differences between the two horizontal principle stresses are small, such as might be expected in a province such as the Colorado Plateau. Delaney and others (1986) presented an expression that must be satisfied, relating the magma pressure the minimum and maximum compressive regional stresses S_h and S_H, respectively, and the clockwise angle α between the normal to the strike of the dike and direction of S_h (Figure 7b). Under these circumstances, relations among maximum crack thickness, crack length, crack orientation, and driving pressures are:

$$
\begin{aligned}
&P_m > S_\alpha \\
&T_{max} = \frac{1}{2}\frac{P_m - S_\alpha}{\mu / (1-\nu)} L \\
&S_\alpha = S - \frac{\Delta S}{2}\cos 2\alpha
\end{aligned}
\tag{2}
$$

where $S = (S_H + S_h)/2$ is the mean horizontal stress and $\Delta S = S_H - S_h$ is the maximum horizontal stress difference (Delaney and others, 1986). $P_m - S_\alpha$ is the difference between magma pressure and mean horizontal regional stress. A dike oriented with $\alpha = 0°$ would have a lesser driving pressure, $P_m - S_h$, than one at $\alpha = 90°$, which would require a greater driving pressure, $P_m - S_H$. If the magma-driving pressure is large in comparison to the horizontal stress difference, then a dike is able to dilate joints of any strike; if the magma-driving pressure is small in comparison to the stress difference, then only joints of a narrow range of strikes would be suitable.

The driving pressure $P_m - S_\alpha$ in equation 2 varies linearly and symmetrically about the crack midplane such that the driving pressure at the crack tip is zero. The horizontal regional stress S_α is resolved from the stresses S_h and S_H and the angle α (Figure 7b). The stress intensity at the crack tip is zero, $K_I = 0$, because the magma flows along a pre-existing fracture. Accordingly, the half-length L of the crack is not constrained by the fracture toughness of the host rock (Delaney and Pollard, 1981).

We plot strikes as a function of maximum thickness measured along the San Rafael dikes (Figure 8b) and found no significant relation among thickness, length and strike; there is no apparent relation to suggest, for instance, that thicker dikes are systematically either longer than others or oriented more optimally than others with respect to the regional stresses.

RELATIVE AGES OF INTERSECTED DIKES

Dikes of northwesterly and northeasterly strikes cut or deflect the other at eight localities (Figure 9). At two of these localities (*c* and *h* in Figure 9), three intersections exist among four dikes. Rotation of the least compressive stress direction during magmatism could cause rotation of strikes of dikes. We show, however, that relative ages of the intersected dikes do not support a rotation of the stress directions.

Mechanical interactions of a later dike intruding near an earlier dike permits their relative ages to be determined. The simplest interaction results when one dike cuts across the other. This relation is not observed at all intersections, however, because of the dikes' segmented forms. A less simple but equally persuasive interaction is the deflection of a later crack caused by the presence of an earlier one (Olson and Pollard, 1989). The deflection is caused both by the presence of a structural inhomogeneity, the dike, and by the stresses produced in the host rocks by its intrusion.

Based on field evidence, intersections at five of the eight localities (*a, b, e, f, and h* in Figure 9) indicate that dikes with northeasterly strikes are younger than those with northwesterly strikes. The two intersections at locality *c* reveal the opposite sense of relative age. Relative ages of dikes were indeterminate at the remaining two localities (*d* and *g*). At locality *c*, the relatively older dike has an 4.6±0.2-Ma age (sample SAL-4, Table 1), suggesting that the younder dike might have been emplaced during the later 3.6-Ma magmatic episode. Indeed, one of the younger, northeasterly striking dikes of locality *h* has ages of 3.4±0.2 and 3.8±0.2 Ma (SAL-2 and SAL-1A, Table 1), consistent with the northwesterly striking dikes being emplaced in the 4.6-Ma episode. Another northeasterly striking dike at locality *h* and the relatively younger dike at locality *e*, however, have age of 4.6±0.2 Ma (SOL-1 and FRY-4, respectively, Table 1). Thus, dike intersections can not reflect changes of emplacement conditions between the million year interval between the two episodes of magmatism. These K-Ar ages are nowhere inconsistent with determinations of relative ages of the intersecting dikes. They do, however, require that some of the intersections were produced during the 4.6-Ma episode.

HOST-ROCK JOINTS AS MAGMA PATHWAYS

No simple relation exists among dike thickness and length (Figures 3, 5, 8a) and dike thickness and strike (Figures 3, 6a, 8b). Moreover, it does not appear from the relations of intersected dikes (Figure 9) that the disparate strikes of the San Rafael dikes can be explained by rotation of the regional stress field during the magmatic interval. We show here that dikes exposed in strata of the San Rafael Group probably acquired their strikes when magma ascended along joints of the underlying rocks of the Glen Canyon Group.

Dikes and joints in the San Rafael Group

Strikes of near-vertical host-rock joints in each unit of the San Rafael Group were compared with strikes of the dikes to test whether magma may have ascended along host-rock joints. We measured only systematic joints, that is, those that are vertically continuous across outcrops and part of a set that is horizontally continuous along much of an outcrop. We took measurements throughout the area of the San Rafael dike swarm to avoid biasing results by concentrating on areas of exceptional exposure. We also avoided taking measurements within about 50 m of dikes because joints there can be caused by stresses associated with intrusion of the dike itself (Delaney and others, 1986).

The distribution of strikes of dikes (Figure 6) does not conform to that of any set of host-rock joints (Figure 10). In general, no unit of the San Rafael Group has a distinctly different distribution of joint strikes than the others. Furthermore, there exists no dominant direction of host-rock jointing; histograms of number versus strike show that many of the joints cluster among directions of about N80–65°W, N40–20°W, and N25–55°E. Many of the dikes parallel the N40–20°W cluster of joints, but the distribution of dike strikes is distinctly different than any portion of the distribution of host-rock joint strikes. The N14°W mean and median strike of the dikes lies within a minimum in the strike distribution of host-rock joints.

We studied a well-exposed locality near Willow Wash (Figure 2) to test whether magma could locally have found a path along particular joints, suitably positioned and oriented. The dikes near Willow Wash are exposed in a 2-km^2 area where joints of two general orientations, N55–20°W and N25–75°E, strike across longitudinally more-or-less continuous outcrops of the Summerville Formation. All dike segments, with the exception of those along the northern outcrops of the westernmost dike (Figure 11a), parallel the more northerly striking joints of the N55–20°W set. We suggest that magma entered, flowed along, and dilated particular joints of this set during intrusion. The westernmost dike is different from the others, however. From north to south, it rotates from a strike of N25°W in an area with nearby parallel joints to N8°W in an area with an absence of such joints. Delaney and others (1986) discussed this area and suggested that the northern section of the westernmost dike probably created its own fracture during propagation. Its strike is probably, therefore, a good indicator of the normal to the local direction of least compressive region stress acting at the time of intrusion.

Rock surfaces in the San Rafael Group are not generally exposed over areas large enough to determine the spatial continuity of joint sets. At one locality, near South Salt Wash (Figure 2), we were able to map dike segments and host-rock joints in well exposed strata of the Entrada Sandstone (Figure 11b). There, strikes of joints vary considerably across distances that are small in comparison to the lengths of most dikes. Moreover, individual joints are not nearly so long as dikes. Some areas of the Entrada Sandstone lack systematic joints altogether. In areas of such discontinuous and irregular jointing, intruding magma must have created many of its own fractures as it formed the dikes.

We conclude that some of the dikes of the San Rafael Group dilated pre-existing joints, at least along part of their length. Apparently, however, most obtained their strikes by some other mechanism.

Dikes and joints in the Navajo Sandstone

Along much of the eastern and southwestern margins of the San Rafael swarm, prominent, extensive joint sets of the Navajo Sandstone parallel nearby dikes. To document these relations, we used aerial photographs to make geologic maps and to measure strikes of joints. Along the westernmost Waterpocket monocline (Figures 2, 12a), joint sets are continuous across distances comparable to dike lengths. Although the joints exhibit a wide range of strikes (Figure 13a), a dominant set, striking between N10°W and N25°E, is approximately parallel to dikes striking between N8°W and N12°E that intruded the nearby Navajo Sandstone and overlying Carmel Formation. Elsewhere, near the southwestern margin of the San Rafael Swell (Figures 2, 12b), dikes also cut the Navajo Sandstone parallel to prominent nearby joints. Strikes of these joint sets range from N80°W to N25°E (Figure 13b), with 80 percent striking through about 60° of azimuth from about N80°W to N20°W. The parallelism between some of the joints and the nearby dikes, which strike between N65°W and N15°W, suggests that they served as pathways for the magma.

Dikes in the Navajo Sandstone, or in the Carmel Formation at localities near exposures of the Navajo Sandstone, strike parallel to nearby joint sets (Figures 12, 13). It appears, therefore, that magma ascended along these joint sets. No dike of the San Rafael swarm is exposed more than about 600 m stratigraphically above the Navajo Sandstone, a distance that is smaller than, but comparable to, the outcrop lengths of most dikes. Strikes of the San Rafael dikes, then, may parallel those of certain joint sets in the massive sandstones of the underlying Glen Canyon Group.

DIRECTIONS OF DIKE PROPAGATION

As dikes dilate, many adjacent segments coalesce, leaving offsets, steps, or ridges along the dike contact (e.g., Figure 14a; Pollard and others, 1975, 1982; Nicholson and Pollard, 1985; Baer and Reches, 1987; Rickwood, 1990; Baer, 1991). These features are mechanically equivalent to hackle and plumose structures observed on joint surfaces (Pollard and Aydin,

1989) or cleavage steps observed in crystals (Broek, 1978, p. 34). Dike-segment offsets parallel the local direction of fracture propagation. For a dike segment to dilate, the direction of magma flow must initially correspond to that of fracture propagation. The overall or eventual direction of magma flow, however, which we assume was chiefly vertical, need not everywhere correspond to fracture-propagation directions.

Most of the San Rafael dikes have plunges of offsets that vary along their length (a range of about 20° is apparent in Figure 14a). Some dikes display two directions at a single outcrop (e.g., Figure 14b, c). Where this is so, one direction invariably parallels bedding. We interpret these two directions to correspond to the local upper and lower edges of the segments before coalescence. The bottom of the segment propagated on top of a bedding plane while the top continued to propagate upward. We envision that where a dike segment ascends above a suitable bedding plane, magma flows laterally on that bed even as it continues to ascend. As nearby dike segments rise to the bedding plane, the fracture coalesces across it, leaving an offset or step.

Where exposures permitted, we studied the structures exposed on dike contacts with their wall rocks, eventually collecting 107 measurements of propagation direction (Figure 15). The directions range from vertical to horizontal and approximately one half of the measurements are less than about 30° from horizontal. Magma apparently makes use of all surfaces of weakness in the host rocks during propagation, including bedding. These results point toward the importance of lateral spreading of the fractures even as they grow upward. The horizontal propagation of the San Rafael dikes differs substantially from the lateral propagation of dikes along volcanic rift zones (Rubin and Pollard, 1987; Walker, 1987). Where rift-zone dikes propagate from high-level magma reservoirs, the San Rafael dikes ascended from great depth.

VERTICAL CHANGE IN DIKE THICKNESS AND LENGTH

As the San Rafael dikes approached the earth's surface they rose through rocks of generally decreasing density. Near the earth's surface, moreover, volatile phases separated from the shonkinite magma to form vesicles present at most localities. Because lithostatic loads generally far exceed tectonic loads and have large vertical gradients, dike form may be expected to vary significantly with depth. Moreover, we might expect that the San Rafael dikes, which are only about a kilometer long, lengthen with depth. Although there are no precise estimate of emplacement depth, elevation serves as an approximation of relative depths among the dikes. Strata of the San Rafael Group vary through about 700 m of elevation, as do the dikes; any elevation-dependent changes in dike thickness or length, therefore, are unlikely to stem from changing host-rock lithologies.

For each unit of the San Rafael Group, dike thicknesses and outcrop lengths were fitted to elevation (Figure 16), assuming that variations in thickness and length are log-normally distributed (Figures 3, 5). For the Carmel Formation, Entrada Sandstone, and Curtis and Summerville Formations, thickness tends to increase upward with gradients of 105, 60, and 129 cm/km, respectively; the best fit to all 236 data is 102 cm/km. Dike-outcrop length tends to increase downward with gradients of 2.4, 0.02, and 5.3 km/km for these same units; the best fit to all 174 data is 2.0 km/km. The sense of change in thickness and length is the same for measurements from each unit of the San Rafael Group. No single linear fit, however, is statistically superior to the model that dike thickness and outcrop length are independent of elevation.

The estimated gradients in thickness are unsustainable through more than several kilometers of dike height. Yet, present outcrops are probably less than several kilometers from the paleosurface and influenced by it; at greater depth, near-surface effects are presumably unimportant. One expects that dike-outcrop lengths should increase downward, as it seems they do.

DILATION OF THE SWARM

Extension

Thicknesses of dikes show no regular variation as a function of distance along the swarm (Figure 16a). This result is somewhat unexpected because there are more dikes, 8 to 16 of them, across the center of the swarm than near the ends (Figure 16b). Dikes cause compression of adjacent rocks and this compression decays to ambient values across distances that are comparable to dike length. If regional stresses remained invariant and there was regional crustal extension during swarm emplacement, then later dikes emplaced near the center of the swarm would require greater magma pressures to attain the same thicknesses as earlier dikes. If magma pressure, on the other hand, remained relatively invariant from one intrusion to the next, then later dikes would be narrower where they invaded near earlier ones.

Probably, invasion of the San Rafael swarm accompanied or caused regional extension across the Colorado Plateau margin; host-rock stresses produced by earlier dikes were apparently relieved before emplacement of later dikes. Across its 30-km wide center, the swarm dilated about 17 m, or 560 μstrain perpendicular to the average N14°W strike of the dikes; if the swarm was emplaced during a million-year interval, then the average extension rate was small, about 0.017 mm/y.

Dilation profile

Because thicknesses of the San Rafael dikes do not vary in a regular fashion along the swarm, by multiplying the number of dikes in sections across the swarm by the 1.05-m mean thickness, we obtain the approximate dilation profile of the swarm (Figure 16b). To examine the manner in which the many dikes of the San Rafael swarm successively intruded to produce the dilation profile, we return to the two-dimensional solution for a pressurized crack in an infinite elastic plate (Figure 7a). If the driving pressure is constant along the crack surface, then the thickness profile $T(x)$s elliptical:

$$T(x) = \frac{P_m - S_h}{\mu / (1 - \nu)} \sqrt{L^2 - 4x^2} \tag{3}$$

(from eq. 8.34, Pollard and Segall, 1987). We fit this equation to the dilation profile of the swarm (dashed line, Figure 16b). Near the ends of the swarm, thicknesses predicted by the model exceed those observed; along the center of the swarm, observed thicknesses exceed those predicted by the model.

We now examine a dilation profile for magma dilating along pre-existing fractures. It can be assumed that the loading varies spatially along the crack so that the tip tapers in such a fashion that the $\mathrm{d}T(x) / \mathrm{d}x = 0$ at the tip (Figure 7b). In this instance, we have

$$T(x) = \frac{1}{2} \frac{P_m - S_\alpha}{\mu / (1 - \nu)} \left(\sqrt{L^2 - 4x^2} - \frac{4x^2}{L} \ln \left| \frac{2x}{L - \sqrt{L^2 - 4x^2}} \right| \right) \tag{4}$$

(eq. 22, Delaney and Pollard, 1981). We fit this equation to the approximate dilation profile of the swarm (solid line, Figure 16b) and find good agreement with the observed dilation profile.

The latter model requires that $(P_m - S_\alpha)(1 - \nu) / \mu \approx 10^{-2}$. For an elastic stiffness of $\mu / (1 - \nu) = 5$ GPa, we obtain an average driving pressure of about 50 MPa. This estimate is almost certainly high because the model assumes that the swarm dilated in a perfectly elastic and otherwise undeforming crust. During the million years of swarm emplacement, each dike probably induced local stresses that were subsequently relaxed by regional crustal extension. Nonetheless, the San Rafael swarm appears to have attained a dilation profile (Figure 16b) consistent with driving pressures that are greatest across the center of swarm, decaying to zero at the ends. This could, in principle, be produced by a gradient in the regional stresses symmetrically disposed about the center of the swarm. More likely, magma pressures were greatest near the center of the swarm and lessened toward the periphery.

DISCUSSION

Dike form and orientation

Dike length, maximum thickness, and strike are not well related by theoretical expressions for dilation of uniformly loaded cracks (equations 1, 2; Figure 8). These properties of the San Rafael dikes likely varied considerably along the ascent path of the magma from its source region. Moreover, outcrop lengths of most dikes are very short in comparison to their presumed heights and gradients in both thickness and outcrop length (Figure 16) are large. Probably, the present exposures lie near their upper, discontinuous peripheries of the dikes and their physical attributes should be expected to exhibit their greatest variability near this complex and intrinsically three-dimensional dike-tip region.

Fracture propagation and magma transport

Because some of the San Rafael dikes flowed along and dilated pre-existing host-rock joints, fracture-propagation directions exposed along dike contacts may bear little relation to the direction that magma advanced along the fracture. Yet, the measured directions of propagation are typically consistent over distances of hundreds of meters (for instance, Figure 14a), much greater than the length scale of most joints. Many of the measurements of subhorizontal propagation (Figure 15), therefore, probably reflect spreading of the dikes even as they propagated upward.

A well-known result for the dilation of an elliptical crack (Broek, 1978, p. 80) in an infinite three-dimensional elastic material suggests why, in a general way, dikes must grow laterally as they ascend. The opening-mode stress intensities K_I^a and K_I^b at the major and minor axes along the elliptic crack plane, a and b, respectively, exhibit the proportionality

$$\frac{K_I^a}{K_I^b} = \sqrt{\frac{b}{a}} \qquad (5)$$

These are the stress intensities that must exceed the tensile fracture toughness of the host rock for crack propagation to occur. As a crack extends along the direction of one axis, the stress intensity increases along the tip of the crack near the perpendicular axis. In the absence of pressure gradients due to the relative weights of magma and host rocks, dikes would have a strong tendency to attain circular shapes if the fracture toughnesses of the host rocks were everywhere similar. In that case, about as many horizontal as vertical propagation directions would be expected around the periphery of a crack.

Yet, the San Rafael dikes must have heights that are much greater than their 1-km outcrop lengths. These heights presumably result from the buoyant force of the magma. The horizontal propagation directions may reflect spreading in response to the difficulties of ascent through less dense host rocks. Lister and Kerr (1991) point out that magma need not be buoyant everywhere along its ascent path; some magma can locally rise above its so-called level of neutral buoyancy so long as body forces averaged over the magma and adjacent rock columns permit. Nonetheless, if a substantial volume of magma is at or above its level of neutral buoyancy, these forces promote lateral propagation.

Breccia bodies and pipes along the San Rafael dikes have vertical contacts, indicating that magma transport in these bodies must also have been vertical. Because flow rates depend greatly on conduit thickness or radius and heat-loss and solidification rates do not (Delaney and Pollard, 1981), these pipes undoubtedly served as the primary conduits of magma upward along the dikes. Most dikes, along much of their surface, are probably hydraulically stagnant very soon after dilation.

State of stress

The northward strikes of the San Rafael dikes are consistent with the 7-to-8-Ma dikes on the Wasatch Plateau (Figure 1; Tingey and others, 1991). The Wasatch dikes strike uniformly slightly east of north, giving an easterly direction of least compressive regional stress consistent with crustal extension in that direction (Thompson and Zoback, 1979). Our examination of the San Rafael swarm offers two estimates of direction of least compressive regional stress. The mean strike of the dikes is N14°W (Figure 6). One section of one dike that propagated in unjointed host rock strikes N8°W (Figure 6a).

Judging from the strikes of the dikes (Figure 6), we estimate that the inequality of equation 2a for dilation of pre-existing fractures is satisfied for $-35° \lesssim \alpha \lesssim 35°$, giving $(P_m - S_\alpha)/\Delta S \gtrsim 0.2$. For a driving pressure $P_m - S_\alpha \approx 1$ MPa, we obtain $\Delta S \lesssim 5$ MPa. At 2-km depth, the mean horizontal stress S might be about 30 MPa, corresponding to 15 MPa/km (McGarr and Gay, 1978) and assuming that horizontal stresses at the earth's surface are sensibly zero on the Colorado Plateau. We estimate, then, that the horizontal stress difference could have been as much as about 15% of the mean horizontal stress. A broader estimate of the range of α is obtained for the entire range of dike strikes, 110°. If dikes strike through a range in excess of 90°, then $(P_m - S_\alpha)/\Delta S \gtrsim 0.5$ and $\Delta S \lesssim 2$ MPa or 5% of the mean stress at 2-km depth.

We estimated that the San Rafael swarm caused about 17 m of dilation (Figure 16) during an interval of about a million years, implying a deformation rate quite modest in comparison to those associated with most plate motions. The lack of correlation between the number of dikes across the swarm and their thickness strongly suggests that stresses imposed upon the host rocks by successive dike intrusions were either accommodated by crustal extension or otherwise relaxed before emplacement of successive dikes.

CONCLUSIONS

We grouped the 1942 dike segments of the San Rafael swarm into 174 dikes on the basis of alignment and proximity along strike (Figure 4). Many of these dikes, now exposed as separate intrusions, almost certainly coalesce at depth to form laterally continuous "parent" dikes. Conversely, the upper peripheries of the parent dikes, of which the present exposure is a representative sample, are discontinuous and irregular in form. Probably, the discontinuous and irregular form was preserved when the dikes stopped propagating after some dike segment at the uppermost periphery either began to feed a sill or vented to initiate an eruption. Whereas the dike-segment geometry allows as many as several hundred discrete intrusions of magma, radiometric ages (Tables 1, 2) allow for as few as two pulses at about 3.7 Ma and

4.6 Ma. If breccia bodies along dikes are characteristic of the subsurface beneath eruptive vents and if dikes exposed so near their paleo-surface must have either vented or fed sills, then we would estimate that swarm emplacement consisted of about 45 intrusive episodes.

Strikes of dikes exposed in strata of the San Rafael Group (Figure 6) were probably acquired as magma flowed along and dilated systematic joints of the underlying massive sandstones of the Glen Canyon Group (Figures 12, 13). Variation in strikes of the dikes is consistent with differences in the magnitudes of the horizontal principal stresses that were small in comparison to the magma-driving pressure, consistent with the setting of the swarm on the Colorado Plateau. Nevertheless, the dominant east-of-north strikes of the dikes provide a robust estimate of the direction of least compressive principal stress, about N75°E, acting at the time of emplacement. Poor agreement between theoretical relations for crack thickness, length, and strike (Figure 8) are attributed to both the irregular three-dimensional form of the San Rafael dikes and the complex mode of emplacement where magma dilated along pre-existing joints in some places and formed its own in others.

Maximum dilation of the San Rafael swarm (Figure 17) amounted to about 17 m and was probably accommodated by crustal extension during the million-year magmatic interval. The form of the dilation profile along the present exposure of the swarm is consistent with a distribution of magma pressure and regional stresses interacting with host rocks of negligible tensile strength. Many of the local fracture-propagation directions of the dikes are nearly horizontal (Figure 15). As the dikes attained greater heights during propagation, they also spread laterally to maintain dike-top stress intensities sufficient to assure continued ascent. Magma in most dike segments of the fracture system probably stagnated; magma flow channeled into portions of the fractures that developed into plugs and necks by brecciation and erosion of wall rocks.

REFERENCES

Baer, G., 1991, Mechanisms of dike propagation in layered rocks and in massive, porous sedimentary rocks: Jour. Geophys. Res., v. 96, p. 11,-911–11,929.

Baer, G., and Z. Reches, 1987, Flow patterns of magma in dikes, Makhtesh Ramon, Israel: Geology, v. 15, p. 569–572.

Broek, D., 1978, Elementary Engineering Fracture Mechanics, Sijthoff and Noordohoff, The Netherlands, 437 p.

Cook, K.L., V. Bankey, D.R. Mabey, and M. DePangher, 1989, Complete Bouger gravity anomaly map of Utah: Utah Geol. Min. Surv. Map 122, scale 1:500,000.

Davis, G.H., 1978, Monocline fold pattern of the Colorado Plateau: Geol. Soc. Am. Mem. 151, p. 215–233.

Delaney, P.T., and D.D. Pollard, 1981, Deformation of host rocks and flow of magma during growth of minette dikes and breccia-bearing intrusions near Ship Rock, New Mexico: U.S. Geol. Surv. Prof. Paper 1202, 61 p.

Delaney, P.T., D.D. Pollard, J.I. Ziony, and E.H. McKee, 1986, Field relations between dikes and joints: emplacement processes and paleostress analysis: Jour. Geophys. Res., v. 91, p. 4920–4938.

Gartner, A.E., 1986, Geometry and emplacement history of a basaltic intrusive complex, San Rafael Swell and Capitol Reef areas, Utah: U.S. Geol. Surv. Open-file Report 86-81, 112 p.

Gartner, A.E., and P.T. Delaney, 1988, Geologic map showing a Late Cenozoic shonkinitic intrusive complex, Emery, Sevier, and Wayne Counties, Utah: U.S. Geol. Surv. Misc. Field Studies Map MF 2052, scale 1:48,000.

Gilluly, James, 1927, Analcite diabase and related alkaline syenite from Utah: Am. Jour. Sci., v. 14, p. 199–211.

Gilluly, James, 1929, Geology and oil and gas prospects of part of the San Rafael Swell and some adjacent areas in eastern Utah: U.S. Geol. Surv. Bull. 806-C, p. 69–130.

Kempton, P.D., J.G. Fitton, C.J. Hawkesworth, and D.S. Omerod, 1991, Isotopic and trace element constraints on the composition and evolution of the lithosphere beneath the southwestern United States: Jour. Geophys. Res., v. 96, p. 13,713–13,735.

Lister, J.R., and R.C. Kerr, 1991, Fluid-mechanical models of crack propagation and their application to magma transport in dykes: Jour. Geophys. Res., v. 96, p. 10,049–10,077.

Mattox, S.R., 1991, Petrology, age, geochemistry, and correlation of the Tertiary volcanic rocks of the Awapa Plateau, Piute, Wayne, and Garfield Counties, Utah: Utah Geol. Min. Surv. Misc. Pub. 91-5, 46 p.

Mattox, S.R., 1994, Geochemistry and tectonic significance of late Cenozoic basalts in the Basin and Range—Colorado Plateau transition zone, Utah: Utah Geol. Assoc. Pub. 23, p. 125–138.

McGarr, A., and N.C. Gay, 1978, State of stress in the earth's crust: Ann. Rev. Earth Planet. Sci., v. 6, p. 405-436.

Nelson, S.T., 1989, Geologic map of the Geyser Peak quadrangle, Wayne and Sevier Counties, Utah: Utah Geol. Min. Surv. Map 114, scale 1:24,000.

Nicholson, R., and D.D. Pollard, 1985, Dilation and linkage of echelon cracks: Jour. Struct. Geol., v. 7, p. 583–590.

Olson, J., and D.D. Pollard, 1989, Inferring paleostresses from natural fracture patterns: a new method: Geology, v. 17, p 345–348.

Pollard, D.D., and A. Aydin, 1989, Progress in understanding jointing over the past century: Geol. Soc. Am. Bull., v. 100, p. 1283–1290.

Pollard, D.D., O.H. Muller, and D.R. Dockstader, 1975, The form and growth of fingered sheet intrusions: Geol. Soc. Am. Bull., v. 86, p. 353–363.

Pollard, D.D., and P. Segall, 1987 Theoretical displacements and stresses near fractures in rock: with applications to faults, joints, veins, dikes, and solution surfaces: *in* Fracture Mechanics of Rock, B.K. Atkinson, *ed.*, Academic Press, London, p. 277–349.

Pollard, D.D., P. Segall, and P.T. Delaney, 1982, Formation and interpretation of dilatant echelon cracks: Geol. Soc. Am. Bull., v. 93, p. 1291–1303.

Rickwood, P.C., 1990, The anatomy of a dyke and the determination of propagation and magma flow directions, *in* Mafic dykes and emplacement mechanisms, A.J. Parker, P.C. Rickwood, and D.H. Tucker, *eds.*, A.A. Balkema, Rotterdam, p. 81–100.

Rubin, A.M., 1993, Tensile fracture of rock at high confining pressure: implications for dike propagation, Jour. Geophys. Res., v. 98, p. 15,919–15,935.

Rubin, A.M., and D.D. Pollard, 1987, Origins of blade-like dikes in volcanic rift zones: U.S. Geol. Surv. Prof. Paper 1350, p. 1449–1470.

Smith, J.F., Jr., L.C. Huff, E.N. Hinrichs, and R.G. Luedke, 1963, Geology of the Capitol Reef area, Wayne and Garfield counties, Utah: U.S. Geol. Surv. Prof. Paper 363, 102 p.

Smith, R.L., and R.G. Luedke, 1984, Potentially active volcanic lineaments and loci in western conterminous United States, *in* Explosive Volcanism: Inception, Evolution and Hazards, Studies in Geophysics, National Academy of Science, Washington, D.C., p. 47–66.

Thompson, G.A., and M.L. Zoback, 1979, Regional geophysics of the Colorado Plateau: Tectonophysics, v. 61, p. 149–181.

Tingey, D.G., E.H. Christiansen, M.G. Best, J. Ruiz, and D.R. Lux, 1991, Tertiary minette and melanephelinite dikes, Wasatch Plateau, Utah: records of mantle heterogeneities and changing tectonics: Jour. Geophys. Res., v. 96, p. 13,529–13,544.

Walker, G.P.L., 1987, The dike complex of Koolau Volcano, Oahu: internal structure of a Hawaiian rift zone: U.S. Geol. Surv. Prof. Paper 1350, p. 961–993.

Williams, J.D., 1983, The petrography and differentiation of a composite sill from the San Rafael Swell region, Utah: M. Sci. Thesis, Arizona State Univ., 123 p.

Williams, P.L., and R.J. Hackman, 1972, Geology of the Salina quadrangle, Utah: U.S. Geol. Surv. Misc. Geol. Inv. Map I 591-A, scale 1:250,000.

Zeitz, I., R. Shuey, and J.R. Kirby Jr., 1976, Aeromagnetic map of Utah: U.S. Geol. Surv. Geophys. Inv. Map GP 970, scale 1:1,000,000.

FIGURE CAPTIONS

1. San Rafael shonkinite dike swarm shown in relation to other melanocratic rocks of the western Colorado Plateau margin, of which the Wasatch Plateau swarm is the closest, and to the St. George volcanic zone, of which the Marysvale volcanic center is the most prominent component. Also shown are the Henry Mountains. After Smith and Luedke (1984), Kempton and others (1991), Tingey and others (1991).

2. Generalized geologic map of the San Rafael area. The San Rafael Group (Js) and the underlying Navajo Sandstone (JTr) of the Glen Canyon Group and the overlying Morrison Formation (Jm) are the host rocks of the San Rafael swarm. Tertiary and Quaternary volcanics of the High Plateaus of Utah include: Tertiary latite and trachybasalt flows (Tla); Tertiary volcanic sediments (Tvs); Tertiary basaltic andesite (Tba); and Quaternary olivine basalt (Qtd). Dikes and sills shown in red. Axes of the Waterpocket and Caineville monoclines are shown as solid lines. Sample locations of radiometric ages are in closed circles. After Williams and Hackman (1972), Gartner and Delaney (1988), Nelson (1989).

3. Dike thickness. Histograms of thickness in Carmel Formation, Entrada Sandstone, and Curtis and Summerville Formations. Also shown are best-fit log-normal distributions.

4. Outcrop pattern of dike segments near Cedar Mountain. Compiled at 1:48,000 scale. The number of dikes or magma-intrusion events that produced the more that 250 dike segments is difficult to determine.

5. Histograms of lengths of dikes and dike segments in Carmel Formation, Entrada Sandstone, and Curtis and Summerville Formations. All data compiled from 1:48,000 scale. a. Segment-oucropt lengths. Also shown is best fit relation between length and

frequency of occurence for lengths up to 1.5 km. b. Dike-outcrop lengths. Best-fit log-normal distribution is also shown.

6. Dike orientation. Histograms of strikes of dikes and of dips of dike segments. The 174 dikes are a qualitative grouping of the 1942 dike segments designated after map compilation at a scale of 1:48,000 Gartner and Delaney (1988). Also shown are best-fit normal distributions.

7. Definition sketches of relations between regional stresses S_h and S_H, dike thickness $T(x)$ as a function of coordinate x, maximum dike thickness T_{max}, and dike half length L. a. Dilation of a dike in unjointed host rock in response to uniform magma pressure P_m. b. Dilation of a dike along a joint oriented at angle α to the direction of least compressive regional stress S_h in response to a axisymmetric linear distribution of magma pressure $P_m(x)$.

8. Dike length (a) and strike (b) as a function of maximum thickness. Error bars are 1σ.

9. Sketch maps of 8 dike-intersection localities labeled *a-h*, identifying relative ages where they are well determined by field relations.

10. Strikes of host-rock joints, San Rafael Group. Histograms of strikes in Carmel Formation, Entrada Sandstone, and Curtis and Summerville Formations.

11. Relations of host-rock joints to nearby dikes. a. Map of dikes and systematic joints exposed in the Summerville Formation, Willow Wash. b. Map of dikes and systematic joints exposed in the Summerville Formation, South Salt Wash. Localities shown in Fig. 2.

12. Relations of dikes to joints in Navajo Sandstone. a. Map of dikes and joints along the Waterpocket monocline. b. Map of dikes and joints near the southwestern margin of the San Rafael Swell. Localities shown in Fig. 2.

13. Strikes of host-rock joints visible on aerial photographs, Navajo Sandstone of the Glen Canyon Group. Histograms from data collected along the Waterpocket monocline and along the western and southwestern margin of the San Rafael Swell. Also shown are strikes of dikes exposed in the Navajo Sandstone or in adjacent overlying Carmel Formation.

14. Offsets and steps along walls of dike-segments. a. Oblique side view showing steps plunging steeply to north; plunges about 20° along length of photograph. b. Oblique side view eastward showing segments offset along bedding planes; lower segment is closer. Top segment shows steeply dipping offsets as well. c. End-on view northward of same dike as b, showing tops and bottoms of dike segments offset on bedding planes.

15. Equal-area lower hemisphere projection of dike-propagation directions.

16. Dike thickness (a) and outcrop length (b) as a function of elevation. Also shown are best-fit lines, assuming that thicknesses and lengths are log-normally distributed.

17. Dike thickness (a) and number of dikes (b) along the San Rafael swarm. Data are projected onto azimuth of N14°W. Solid line in (a) is log-normal mean thickness and dashed lines are ±2 log-normal standard deviations. Because dike thickness does not vary along the swarm, the number of dikes across the swarm is proportional to the total swarm dilation. Solid line in (b) is best-fit theoretical shape of dilation along an existing fracture, equation 4 in text. Dashed equation line in (b) is best-fit theoretical shape of dilation along a dike-created fracture, equation 3 in text.

Table 1: K-Ar Radiometric Ages of Shonkinite Dikes

Sample	Longitude Latitude	Material Dated	K_2O (%)	$^{40}Ar^*$ (10^{-11} mole/g)	$^{40}Ar^* / ^{40}Ar^{tot}$	Apparent Age (Ma)
FRY-4 [1]	111° 05' 07" 38° 36' 32"	biotite	8.73	5.880	27.3	4.62 ± 0.15
SAL-4 [2]	111° 07' 45" 38° 34' 30"	biotite	7.93	5.243	29.3	4.59 ± 0.15
SOL-1 [2]	111° 15' 14" 38° 30' 45"	whole rock	2.96	1.995	29.2	4.68 ± 0.26
		less olivine	2.97	1.978	42.5	4.62 ± 0.25
SAL-1A [2,3]	111° 14' 12" 38° 30' 25"	whole rock	3.02	1.652	25.6	3.80 ± 0.25
SAL-2 [2,3]	111° 13' 10" 38° 32' 18"	whole rock	2.71	1.332	25.2	3.42 ± 0.23

K-Ar constants: $\lambda\beta = 4.962 \times 10^{-10}$ yr^{-1}
$\lambda\varepsilon + \lambda\varepsilon' = 0.581 \times 10^{-10}$ yr^{-1}
$^{40}K/K = 1.67 \times 10^{-4}$ mole/mole

[1] Age analysis by U.S Geological Survey, Menlo Park, California.
[2] Age analysis by U.S. Geological Survey, Denver, Colorado.
[3] Samples collected from the same dike, see intersection locality *h* in Fig. 9.

Table 2: K-Ar and $^{40}Ar/^{39}Ar$ Radiometric Ages

Sample	Longitude Latitude	Material Dated	Method	Apparent Age (Ma)	Reference
Shonkinite breccia body near Cathedral Junction	111° 19' 02" 38° 31' 06"	whole rock	K-Ar	3.8 ± 0.2	Delaney et al., 1986
Trachybasalt flow near Hogan Pass	111° 28' 06" 38° 35' 57"	whole rock	K-Ar	3.8 ± 0.2	Delaney et al., 1986
Syenite sill at Table Mountain	111° 05' 47" 38° 32' 38"	biotite	K-Ar	4.6 ± 0.2	Delaney et al., 1986
Basaltic andesite from vent on Thousand Lake Mountain	111° 28' 42" 38° 25' 00"	whole rock	K-Ar	6.4 ± 0.4	Delaney et al., 1986
Shonkinite dike, IRE-2	111° 06' 54" 38° 37' 58"	whole rock	$^{40}Ar/^{39}Ar$	6.60 ± 0.68	Tingey et al., 1991
Shonkinite dike, SOL-3	111° 15' 05" 38° 30' 39"	whole rock	$^{40}Ar/^{39}Ar$	5.17 ± 0.38	Tingey et al., 1991

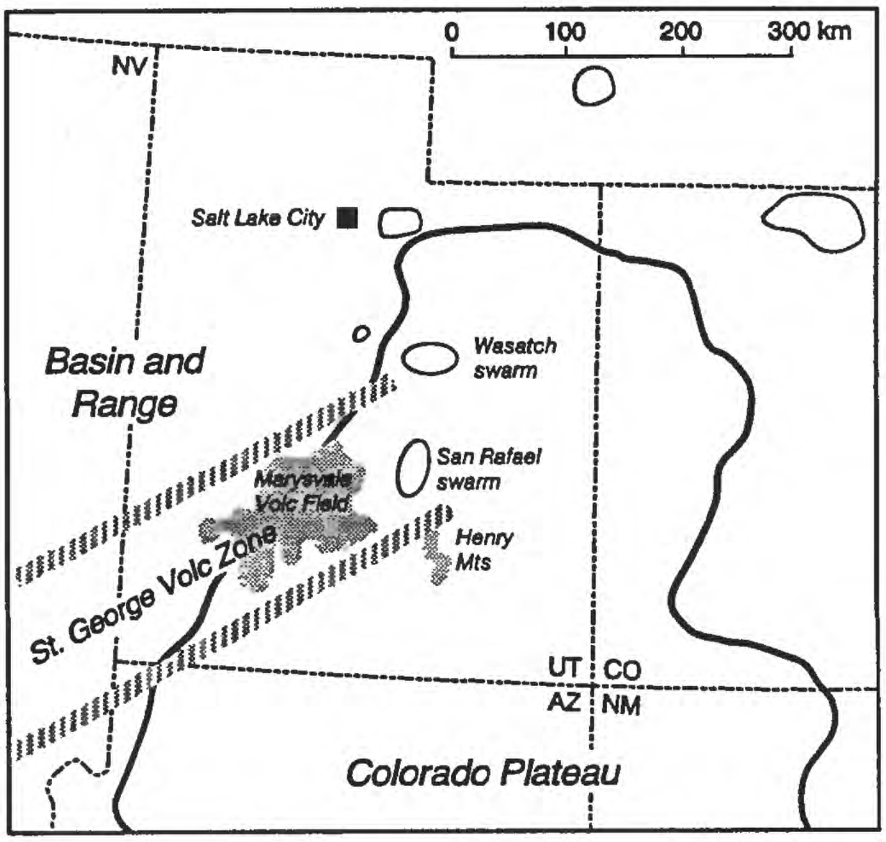
0
100
200
300 km
NV
Salt Lake City
Wasatch swarm
Basin and Range
San Rafael swarm
Marysvale Volc Field
Henry Mts
St. George Volc Zone
UT
CO
AZ
NM
Colorado Plateau

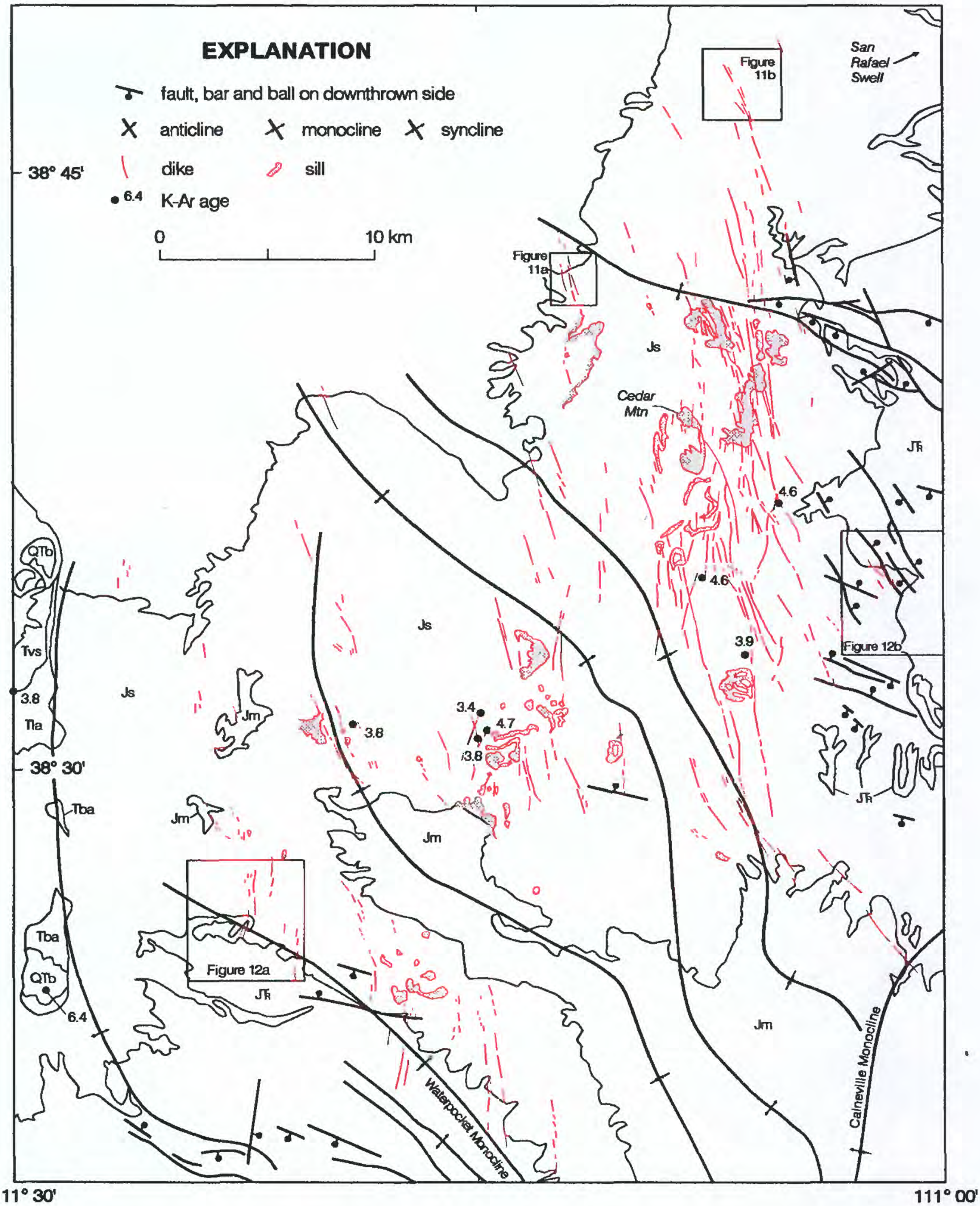
EXPLANATION
fault, bar and ball on downthrown side
anticline
monocline
syncline
dike
sill
6.4
K-Ar age
0
10 km
38° 45'
38° 30'
111° 30'
111° 00'
Figure 11a
Figure 11b
Figure 12a
Figure 12b
San Rafael Swell
Cedar Mtn
Js
Jm
JTR
QTb
Tvs
Tla
Tba
3.8
6.4
4.6
4.6
3.9
3.4
4.7
3.8
3.8
Waterpocket Monocline
Caineville Monocline

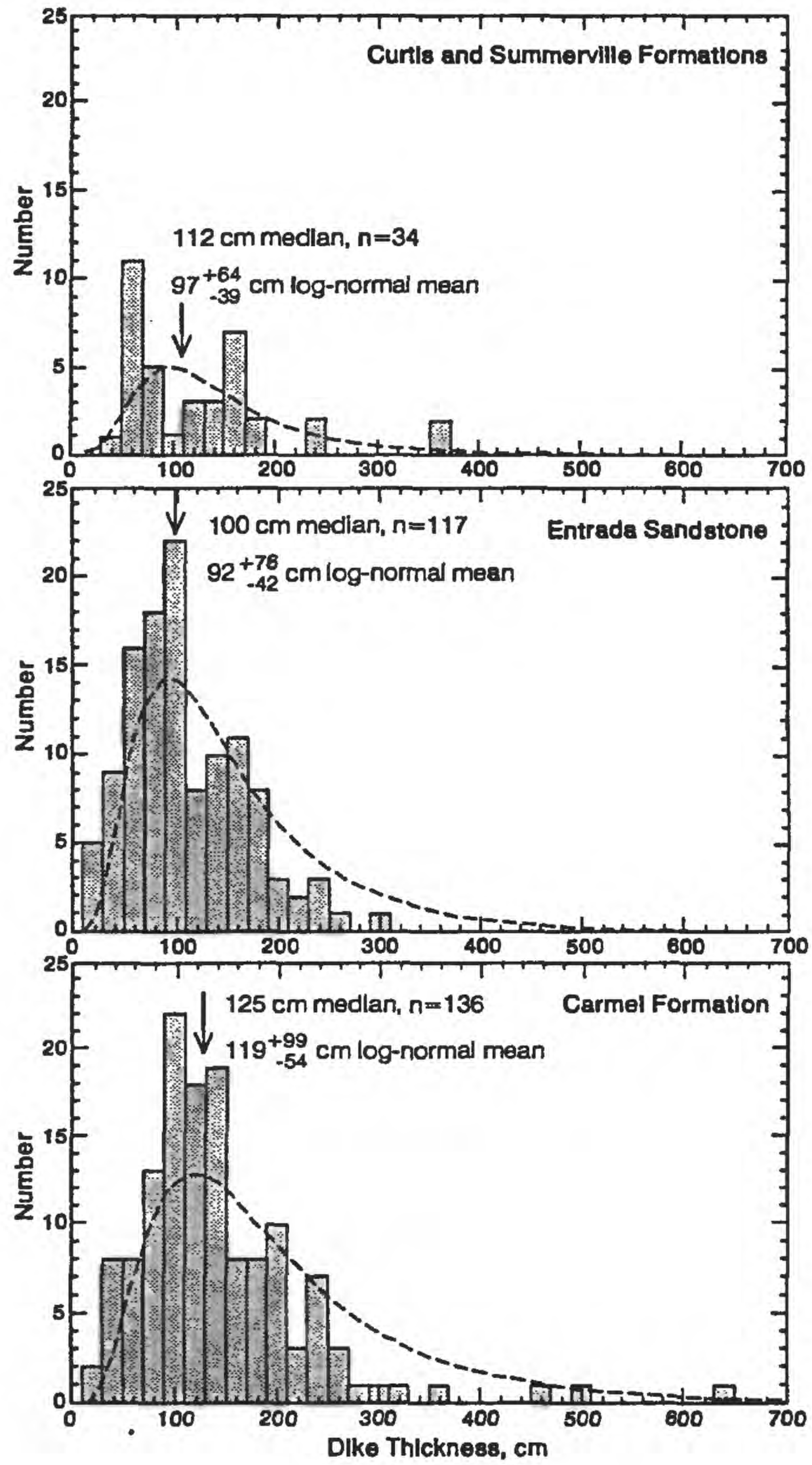
Curtis and Summerville Formations
112 cm median, n=34
97^{+64}_{-39} cm log-normal mean
Entrada Sandstone
100 cm median, n=117
92^{+76}_{-42} cm log-normal mean
Carmel Formation
125 cm median, n=136
119^{+99}_{-54} cm log-normal mean
Number
Dike Thickness, cm
0
100
200
300
400
500
600
700
0
5
10
15
20
25

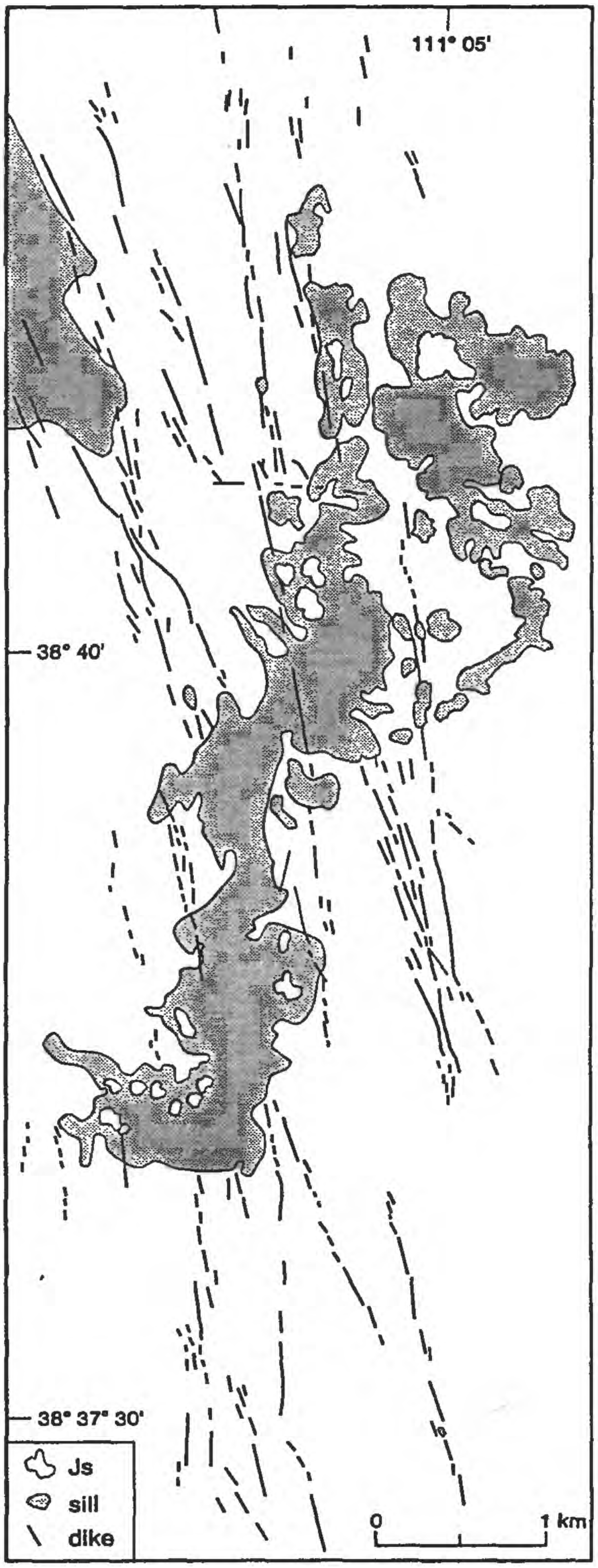
111° 05'
38° 40'
38° 37' 30'
Js
sill
dike
0
1 km

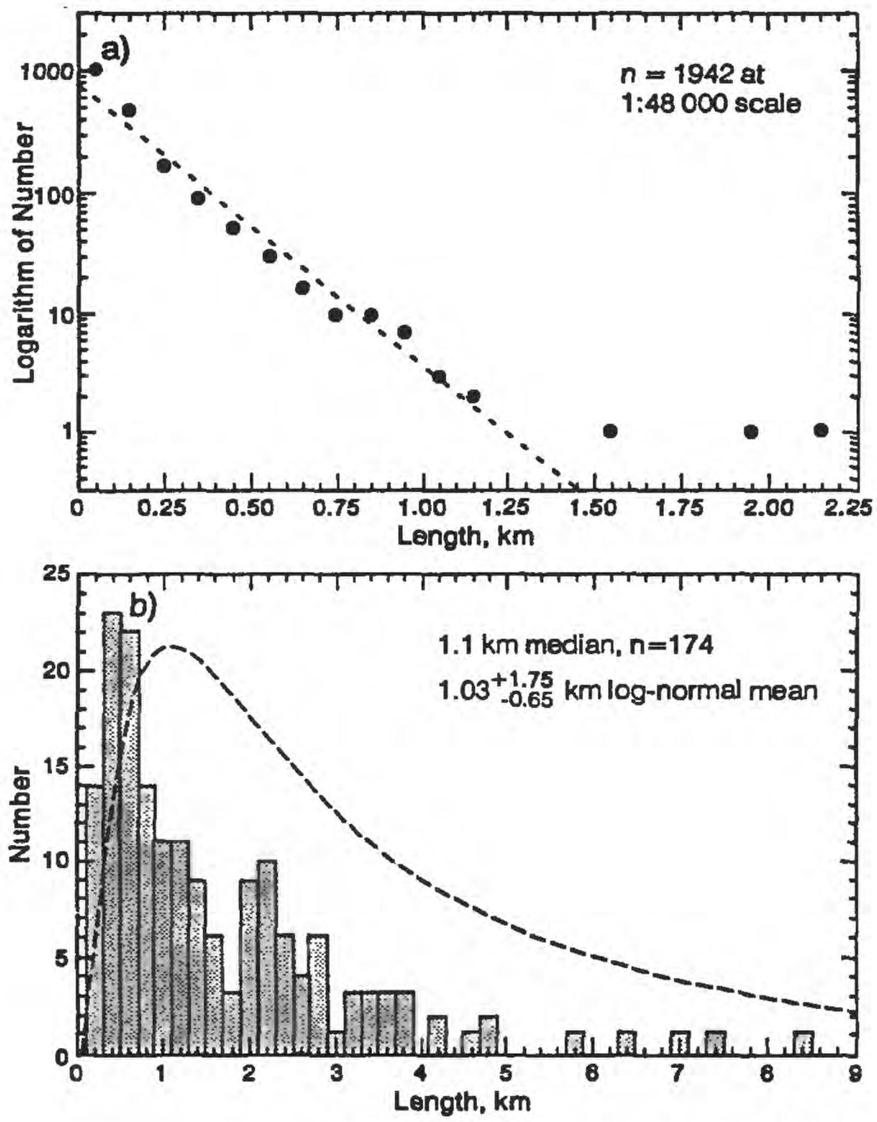
a)
n = 1942 at
1:48 000 scale
Logarithm of Number
Length, km
b)
1.1 km median, n=174
$1.03^{+1.75}_{-0.65}$ km log-normal mean
Number
Length, km

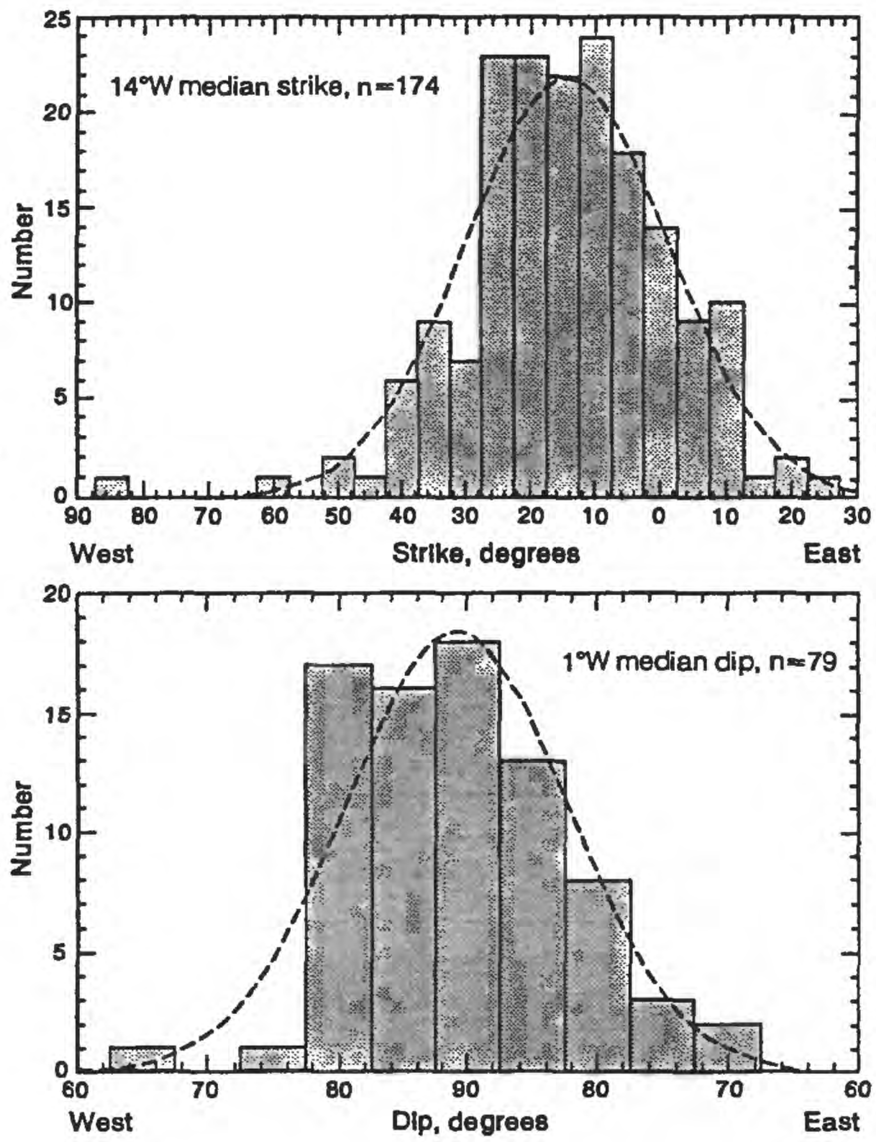
14°W median strike, n=174
Number
Strike, degrees
West
East
1°W median dip, n=79
Number
Dip, degrees
West
East

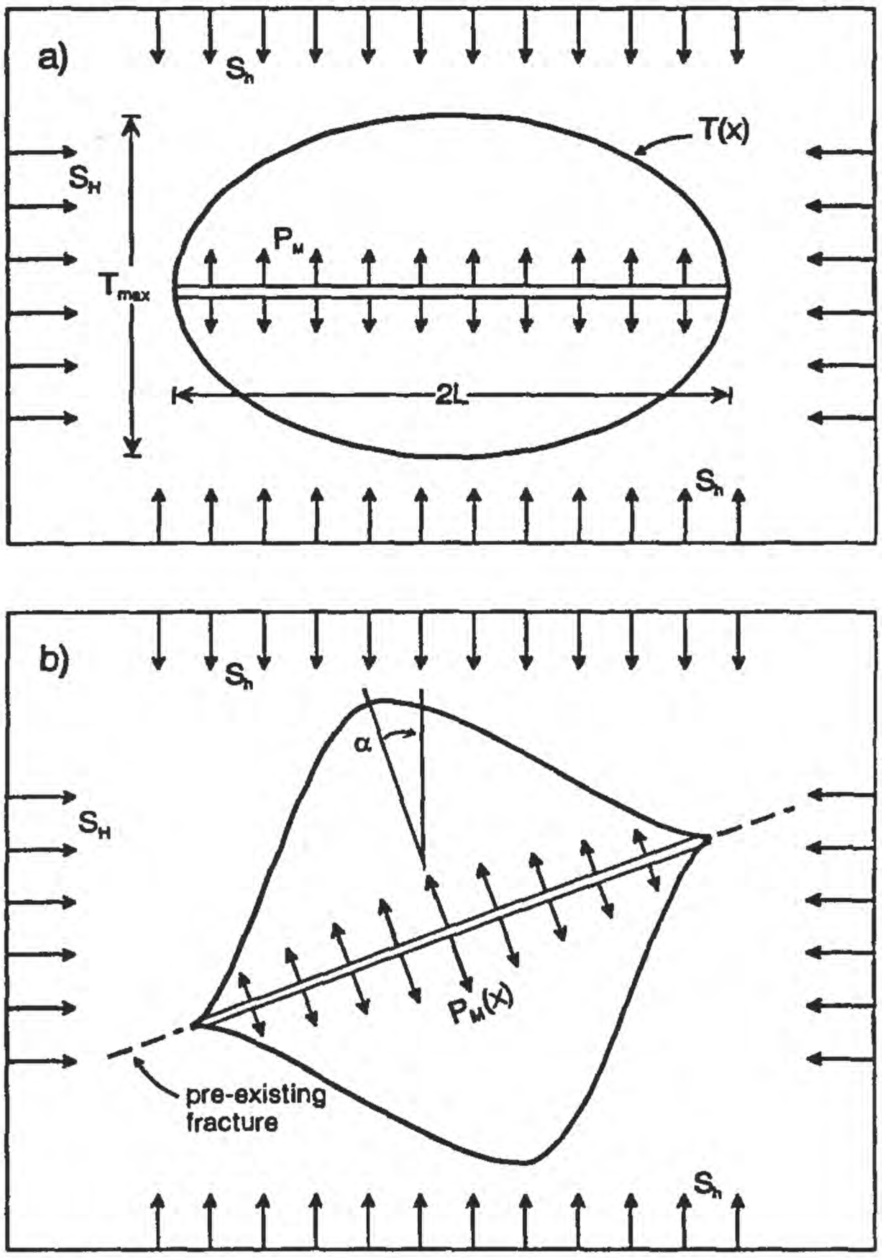
a)
S_h
T(x)
S_H
P_M
T_{max}
2L
S_h
b)
S_h
α
S_H
$P_M(x)$
pre-existing
fracture
S_h

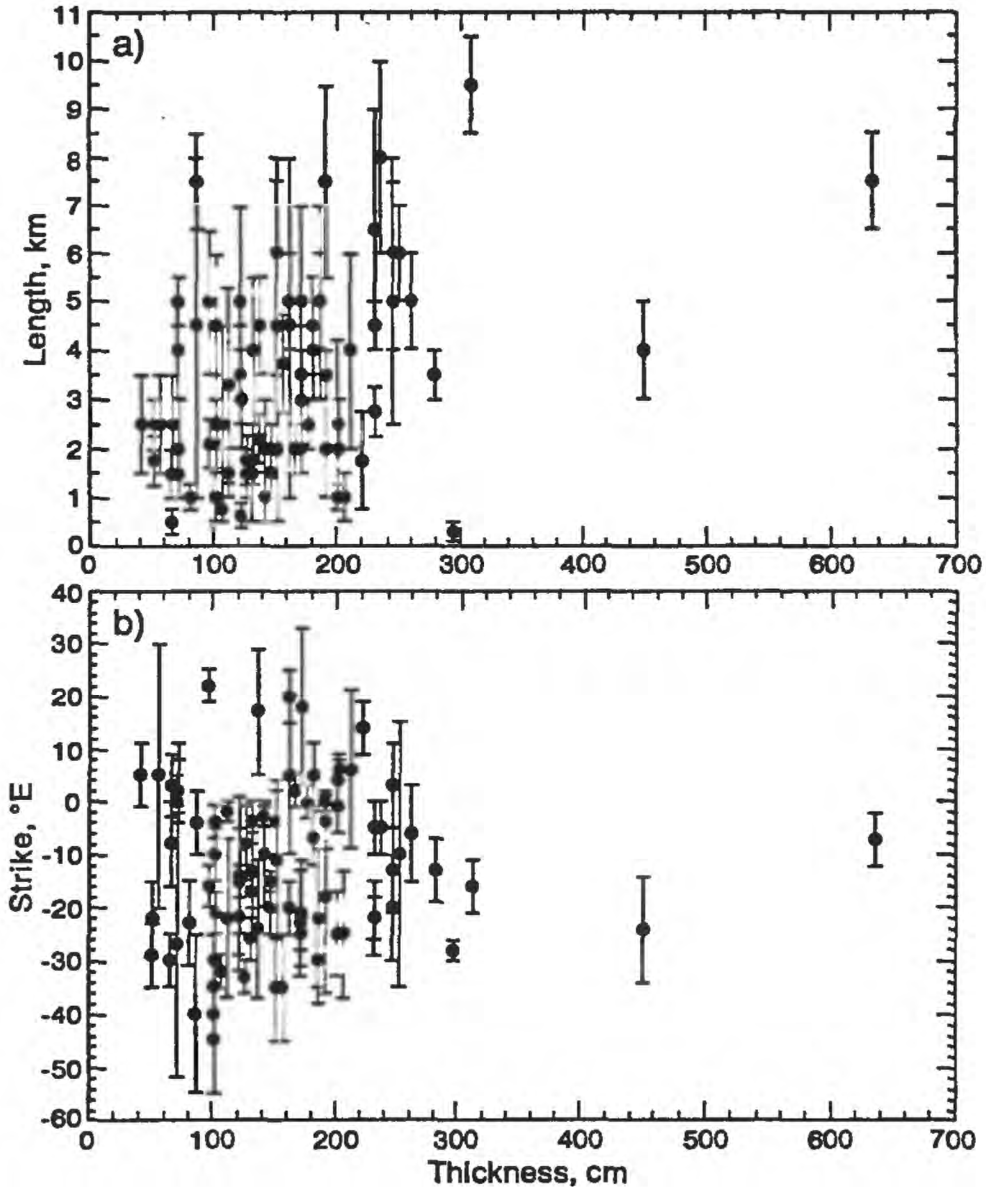
a)
Length, km
b)
Strike, °E
Thickness, cm

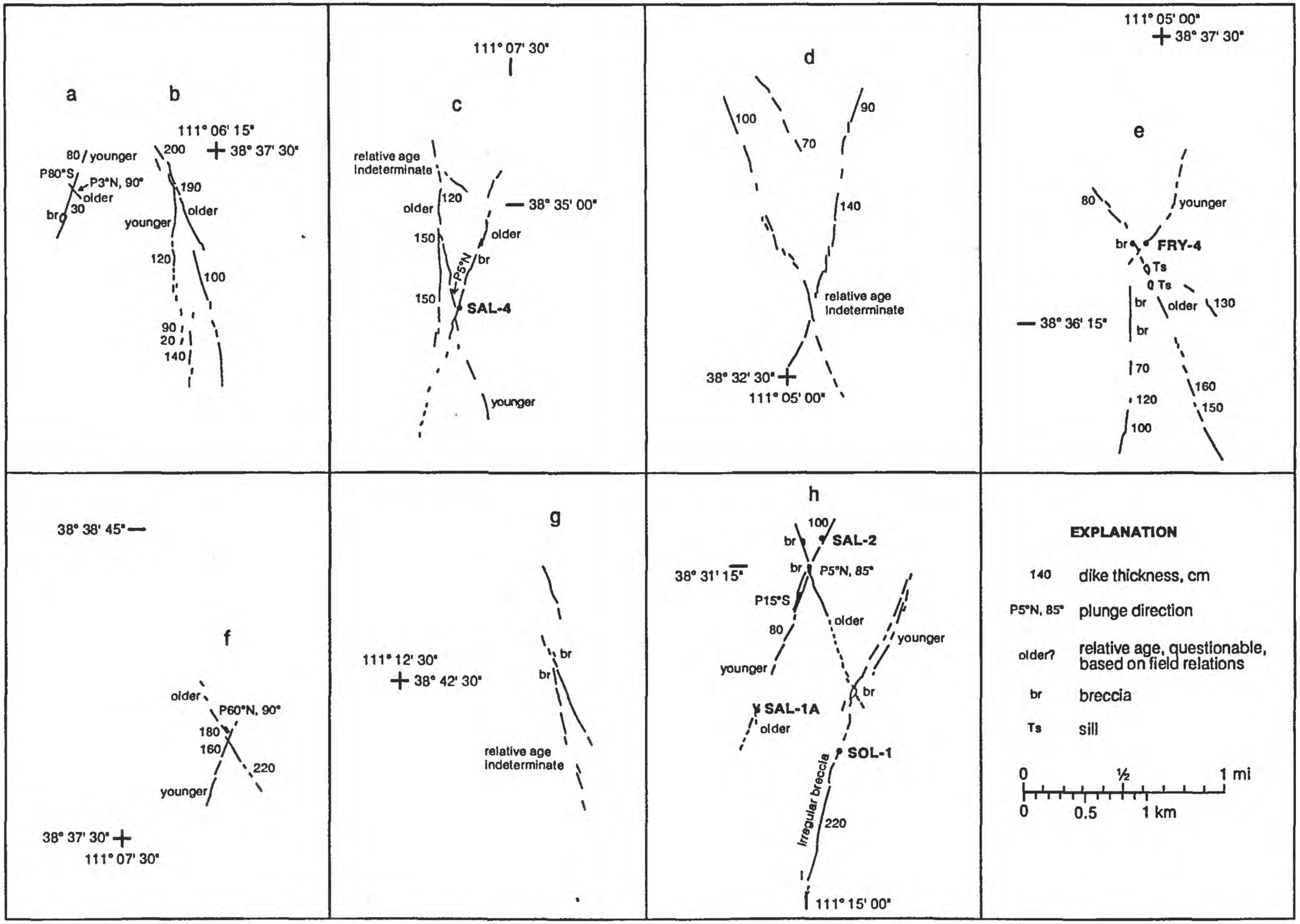
a
b
111° 06' 15"
38° 37' 30"
80 / younger
P80°S
P3°N, 90°
older
br
30
200
190
older
younger
120
100
90
20
140
111° 07' 30"
c
relative age
indeterminate
older
120
38° 35' 00"
150
older
P5°N
br
150
SAL-4
younger
d
100
70
90
140
relative age
indeterminate
38° 32' 30"
111° 05' 00"
111° 05' 00"
38° 37' 30"
e
80
younger
br
FRY-4
Ts
0 Ts
br
older
130
38° 36' 15"
br
70
160
120
150
100
38° 38' 45"
f
older
P60°N, 90°
180
160
220
younger
38° 37' 30"
111° 07' 30"
g
111° 12' 30"
38° 42' 30"
br
br
relative age
indeterminate
h
100
br
SAL-2
38° 31' 15"
br
P5°N, 85°
P15°S
older
80
younger
younger
br
SAL-1A
older
SOL-1
irregular breccia
220
111° 15' 00"
EXPLANATION
140 dike thickness, cm
P5°N, 85° plunge direction
older? relative age, questionable, based on field relations
br breccia
Ts sill
0 ½ 1 mi
0 0.5 1 km

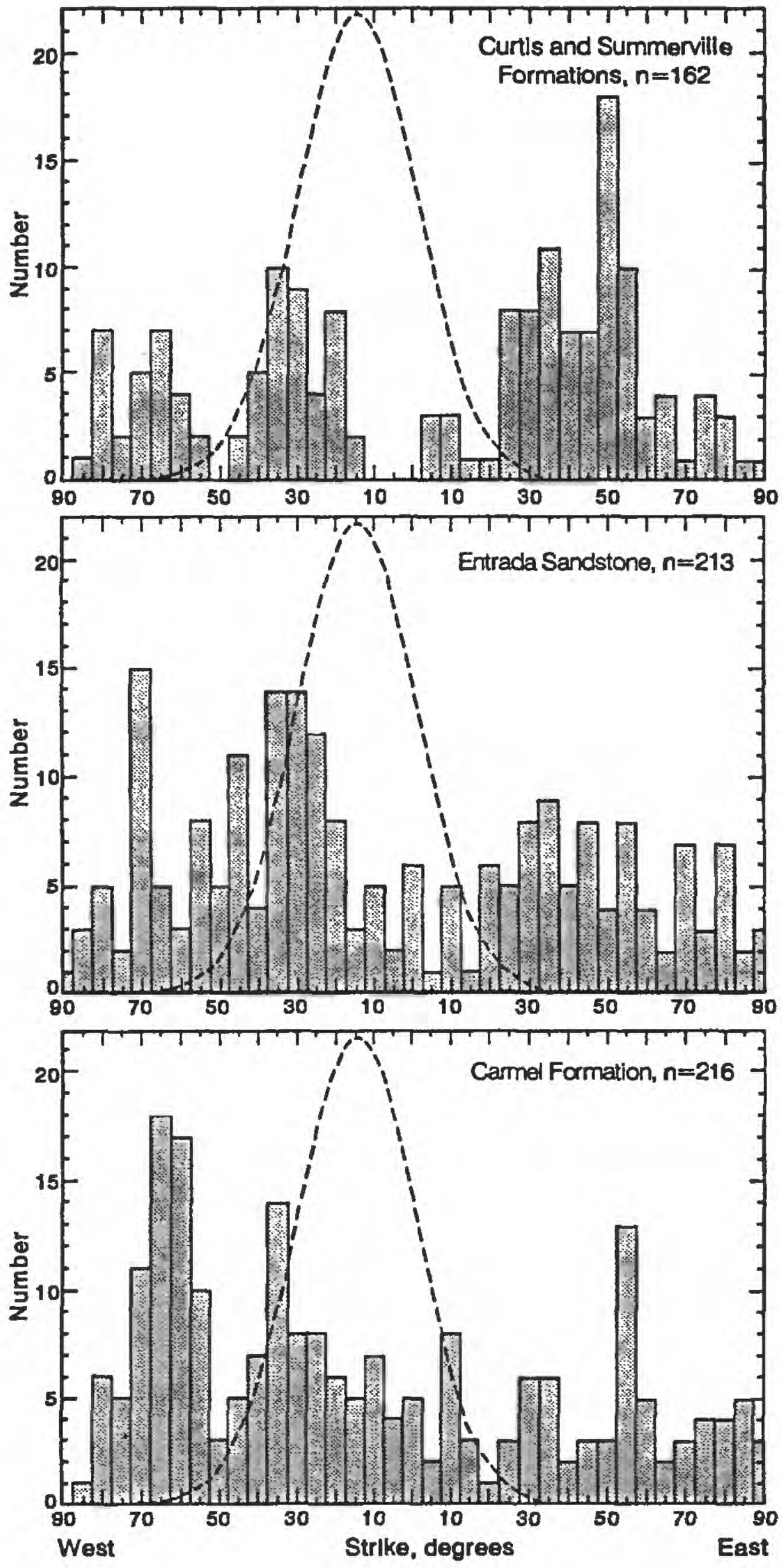
Curtis and Summerville Formations, n=162
Entrada Sandstone, n=213
Carmel Formation, n=216
Number
0
5
10
15
20
90
70
50
30
10
10
30
50
70
90
West
Strike, degrees
East

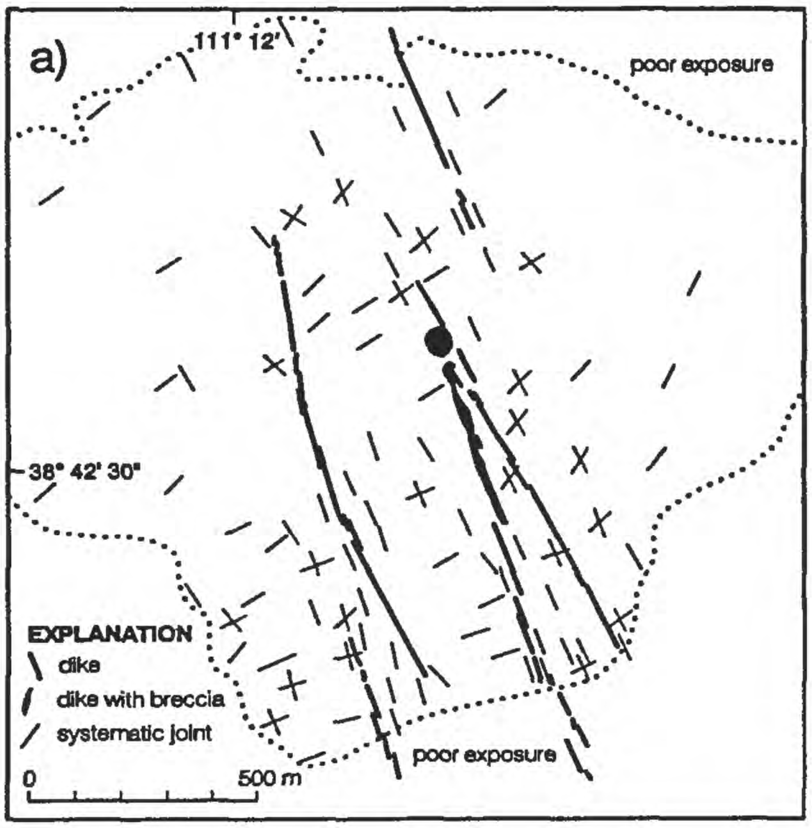
a)
111° 12'
poor exposure
38° 42' 30"
EXPLANATION
dike
dike with breccia
systematic joint
0
500 m
poor exposure

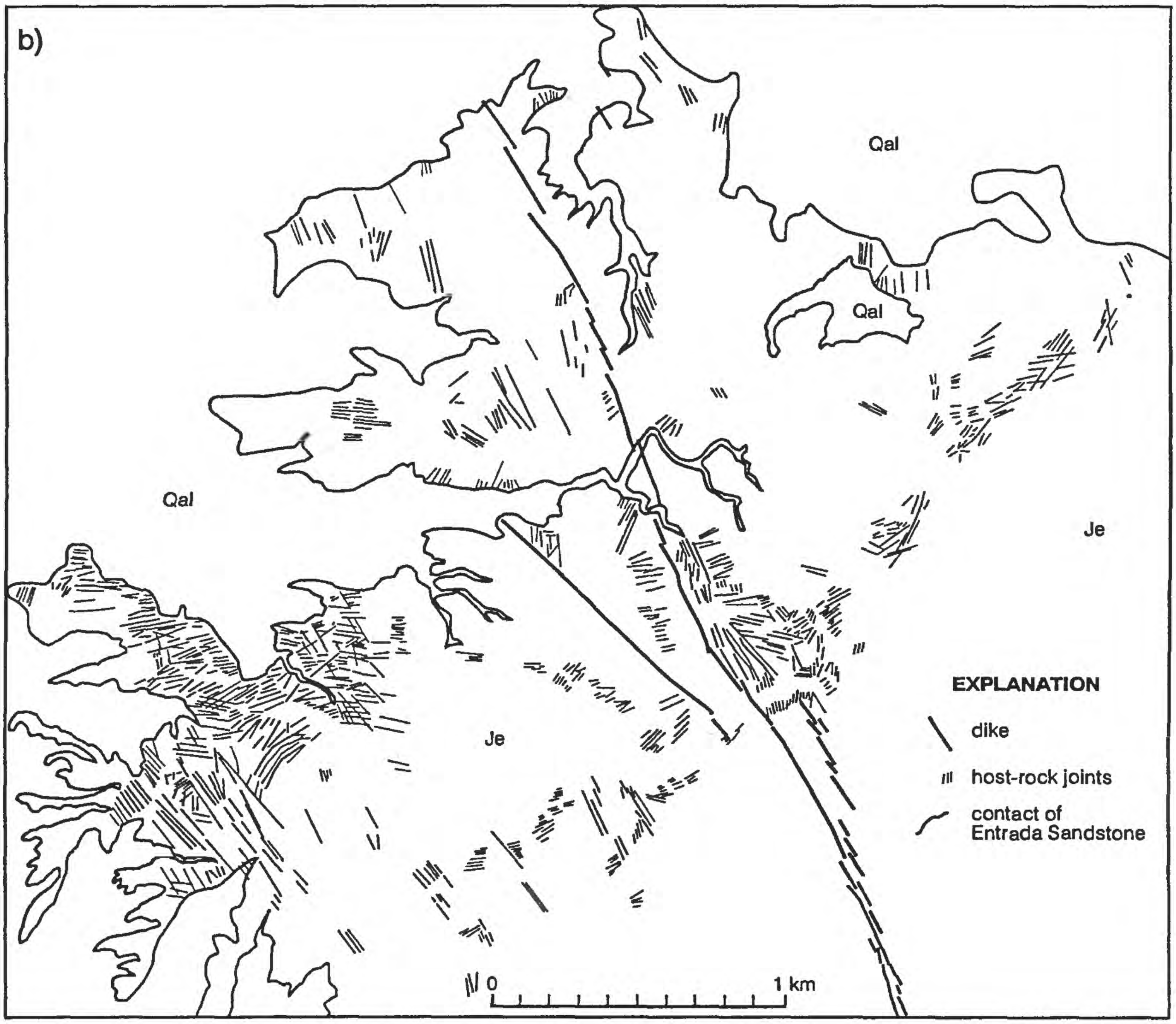
b)
Qal
Qal
Qal
Je
Je
EXPLANATION
dike
host-rock joints
contact of
Entrada Sandstone
N
0
1 km

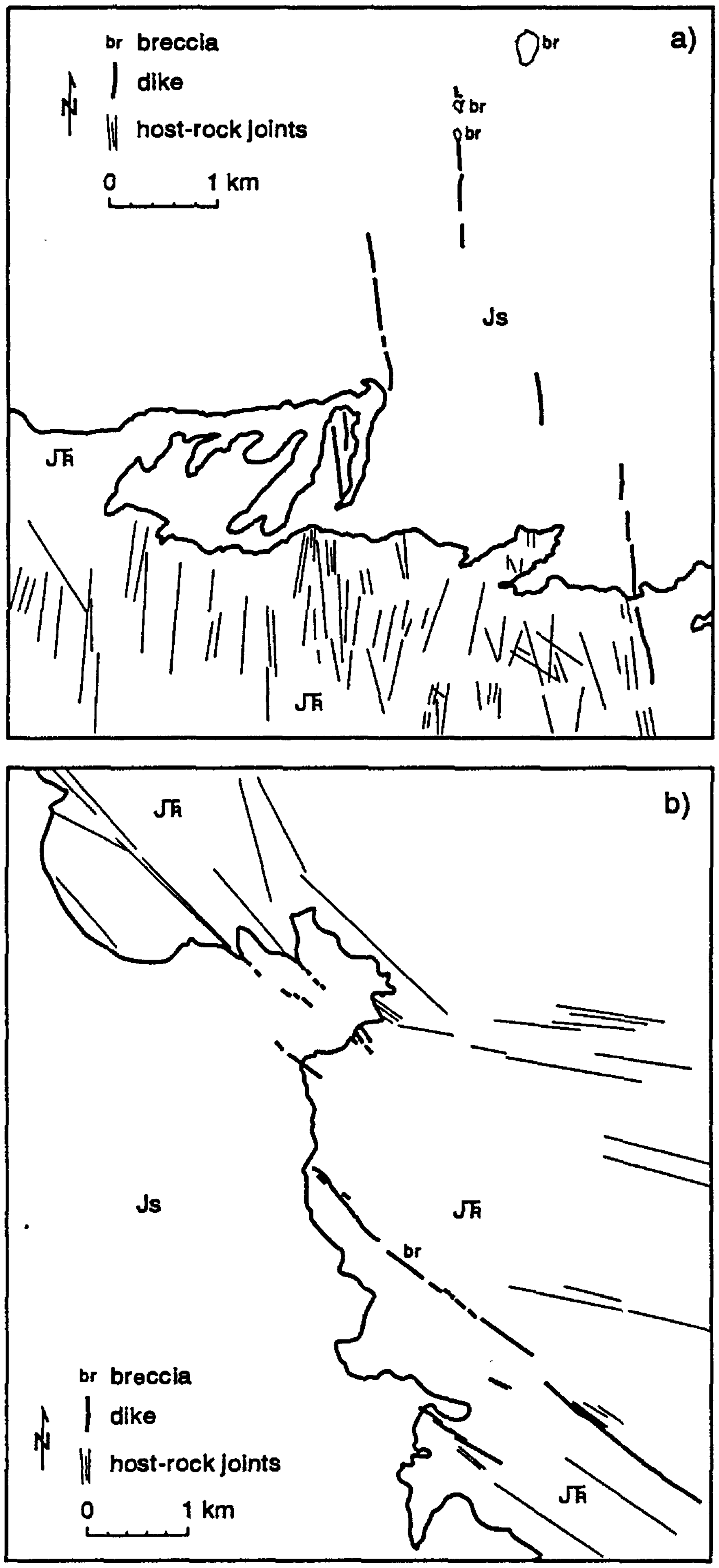
a)
br breccia
dike
host-rock joints
0 1 km
br
br
br
Js
JTR
JTR
b)
JTR
Js
JTR
br
br breccia
dike
host-rock joints
0 1 km
JTR

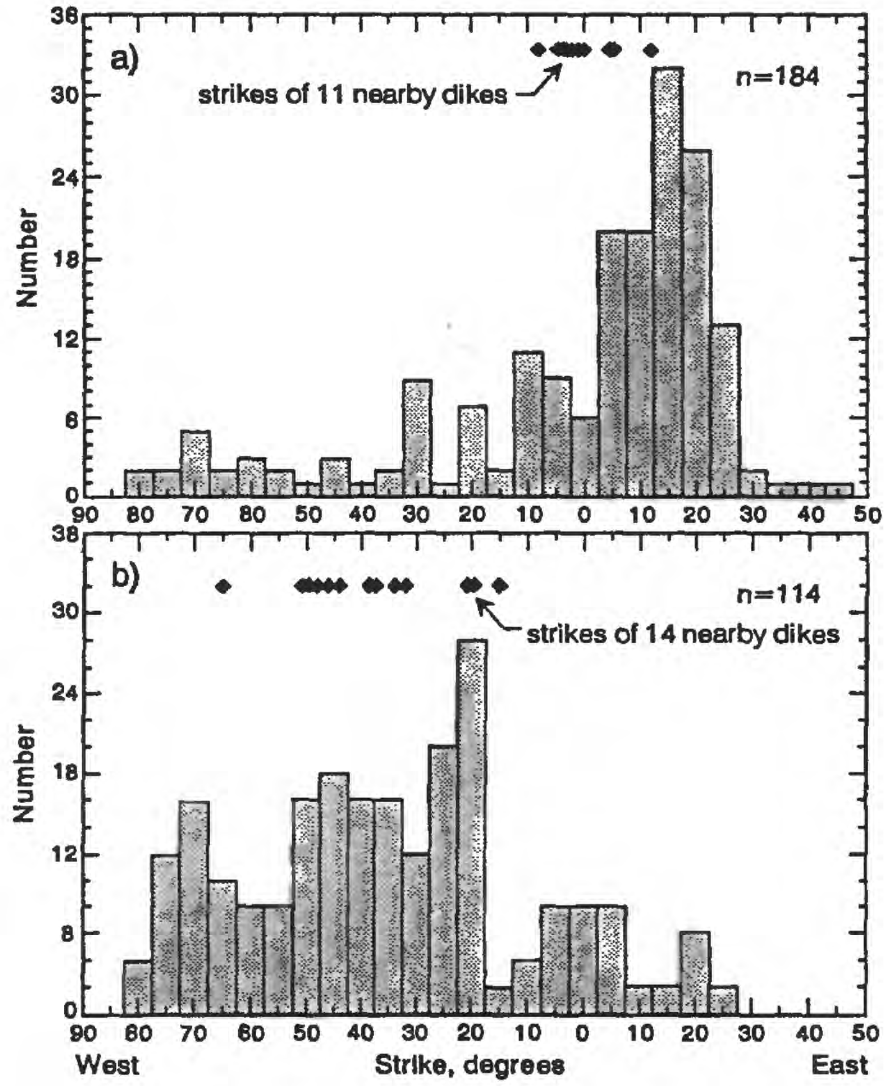
a)
strikes of 11 nearby dikes
n=184
b)
n=114
strikes of 14 nearby dikes
Number
Number
West
Strike, degrees
East

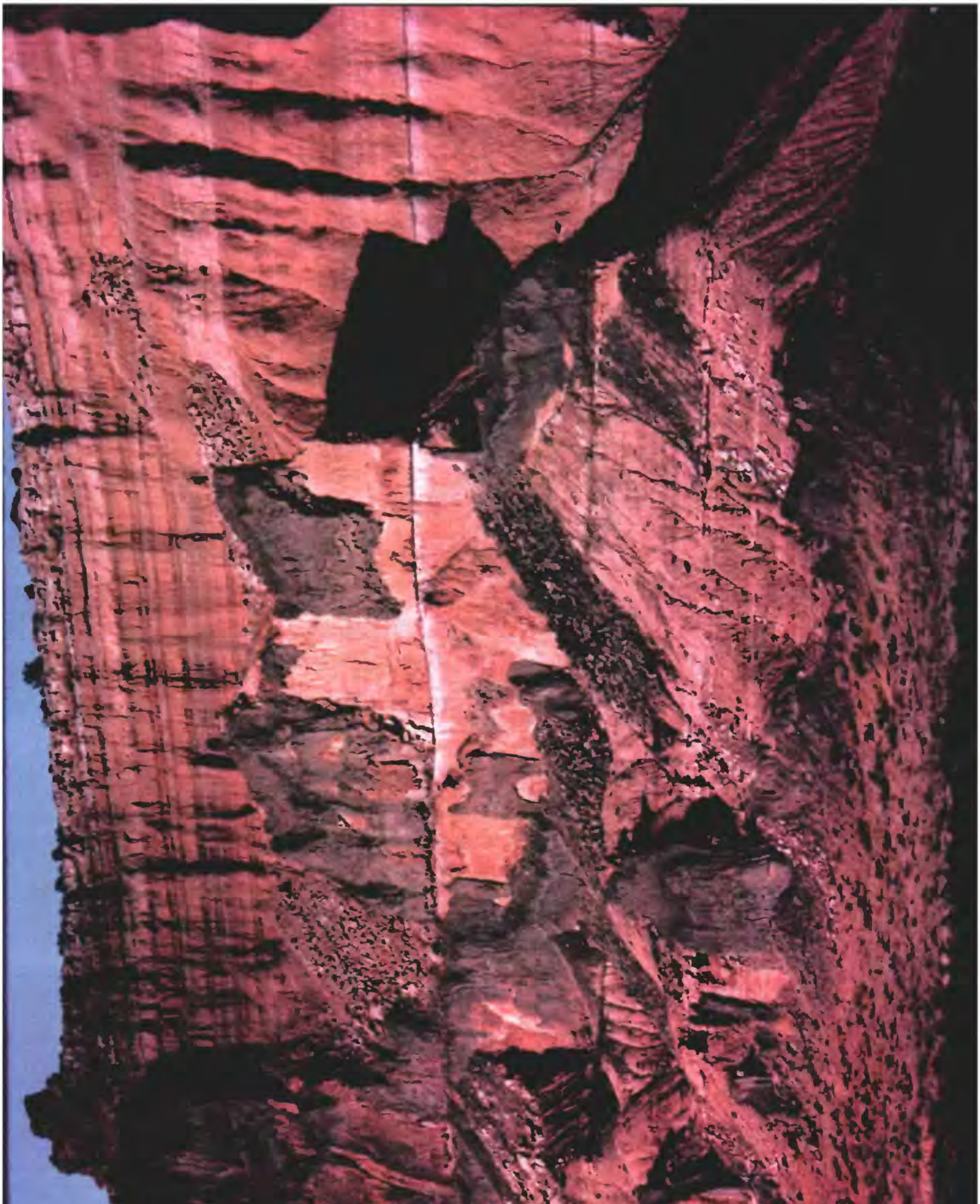

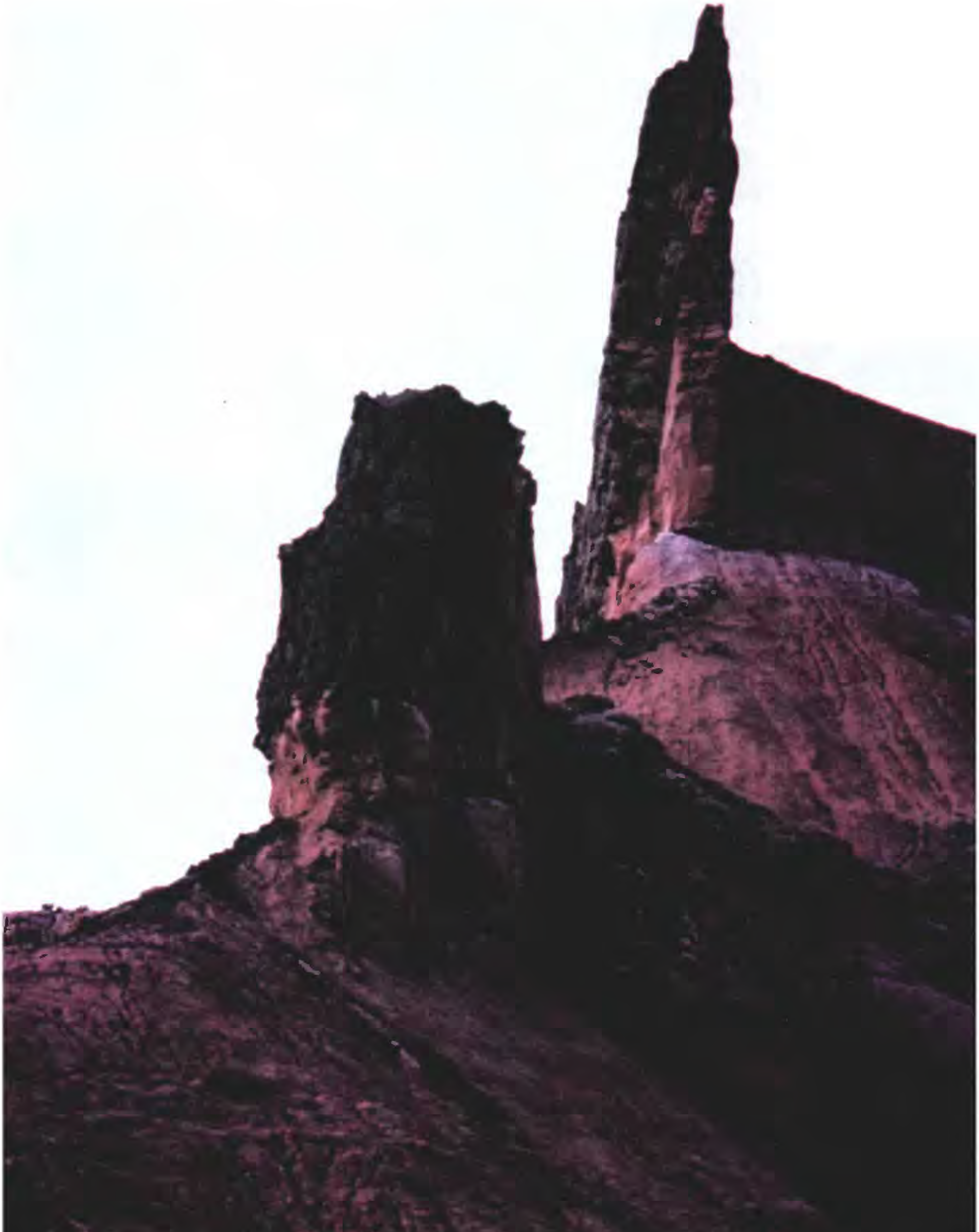

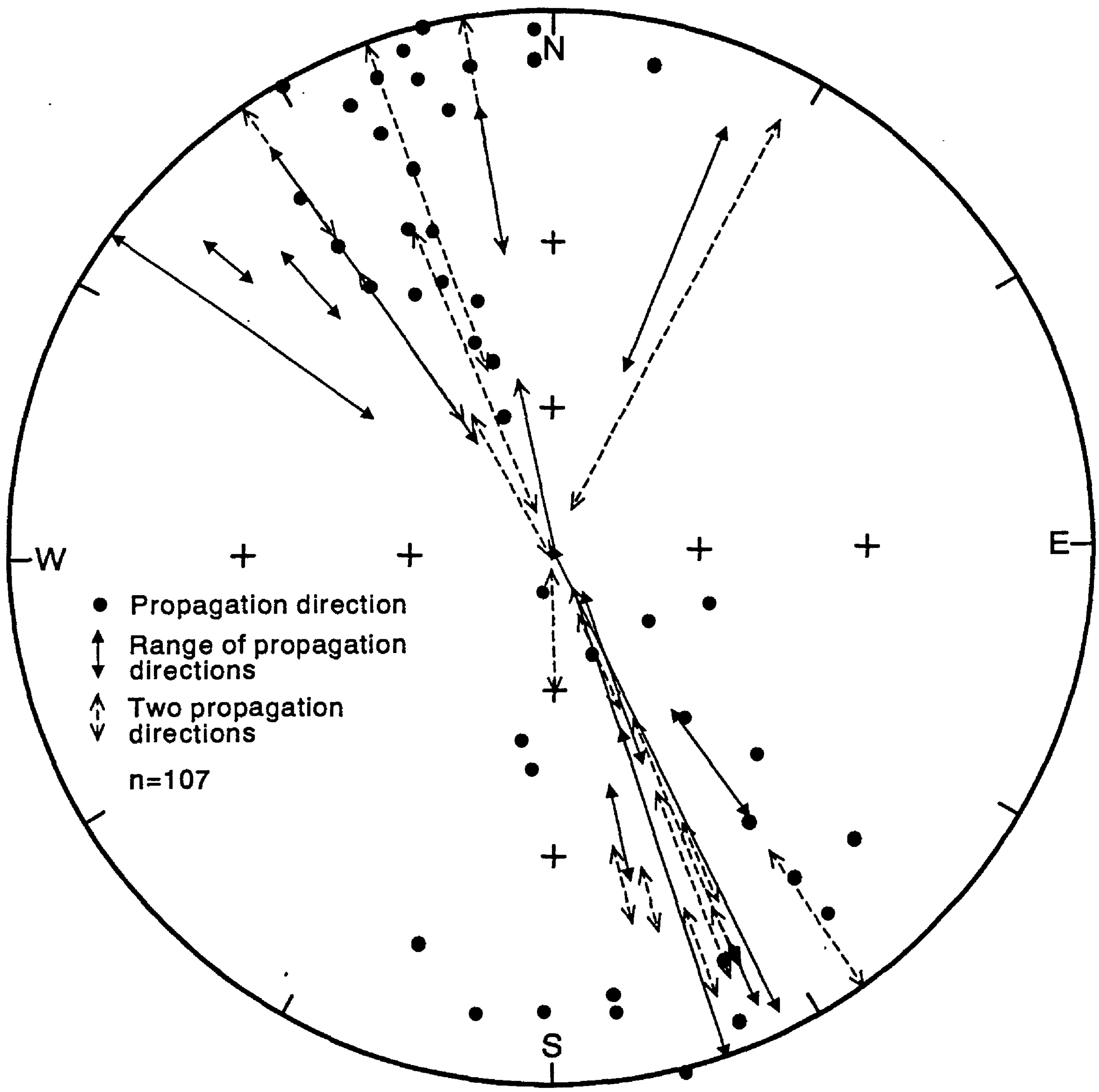
N
E
S
W
Propagation direction
Range of propagation directions
Two propagation directions
n=107

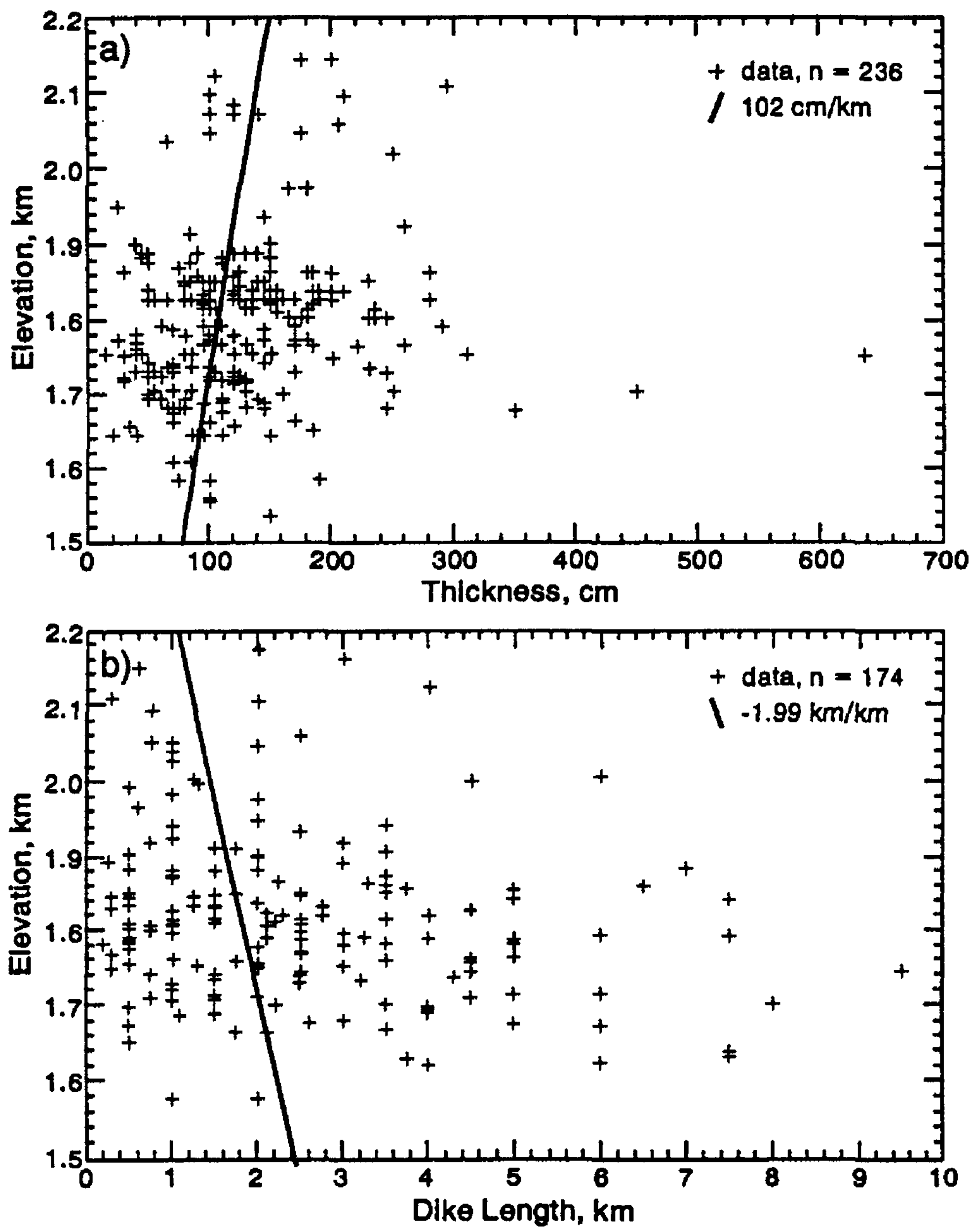
a)
+ data, n = 236
102 cm/km
Elevation, km
Thickness, cm
b)
+ data, n = 174
-1.99 km/km
Elevation, km
Dike Length, km

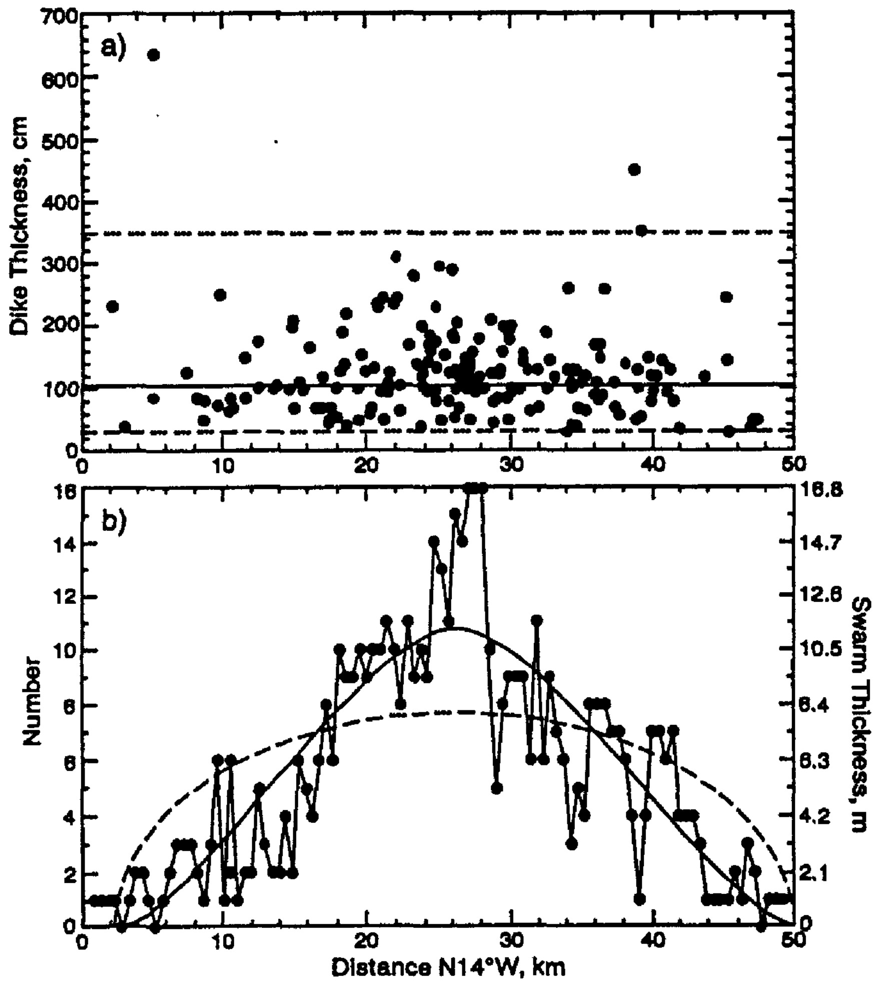
a)
b)
Dike Thickness, cm
Number
Swarm Thickness, m
Distance N14°W, km